A bipartite transcription factor module controlling expression in the bundle sheath of *Arabidopsis thaliana*

Patrick J. Dickinson[1*], Jana Kneřová[1*], Marek Szecówka[1], Sean R. Stevenson[1], Steven J. Burgess[1], Hugh Mulvey[1], Anne-Maarit Bågman[2], Allison Gaudinier[2], Siobhan M. Brady[2] and Julian M. Hibberd[1]

[1]Department of Plant Sciences, Downing Street, University of Cambridge, Cambridge CB2 3EA, UK.

[2]Department of Plant Biology and Genome Center, University of California, Davis, CA 95616, USA

PJD - pd373@cam.ac.uk

JK - j.knerova@gmail.com

MS - szecowka@protonmail.com

SRS - srs62@cam.ac.uk

SJB - sburgess011@gmail.com

HM - hughmulvey@gmail.com

AMB - ambagman@ucdavis.edu

AG - agaudinier@berkeley.edu

SMB - sbrady@ucdavis.edu

JMH (corresponding) - jmh65@cam.ac.uk

* These authors contributed equally

Abstract

C_4 photosynthesis evolved repeatedly from the ancestral C_3 state, improving photosynthetic efficiency by ~50%. In most C_4 lineages photosynthesis is compartmented between mesophyll and bundle sheath cells but how gene expression is restricted to these cell types is poorly understood. Using the C_3 model *Arabidopsis thaliana* we identified *cis*-elements and transcription factors driving expression in bundle sheath strands. Upstream of the bundle sheath preferentially expressed *MYB76* gene we identified a region necessary and sufficient for expression containing two *cis*-elements associated with the MYC and MYB families of transcription factors. *MYB76* expression is reduced in mutant alleles for each. Moreover, down-regulated genes shared by both mutants are preferentially expressed in the bundle sheath. Our findings are broadly relevant for understanding the spatial patterning of gene expression, provide specific insights into mechanisms associated with evolution of C_4 photosynthesis and identify a short tuneable sequence for manipulating gene expression in the bundle sheath.

Introduction

A fundamental characteristic of multicellular eukaryotes is the ability to carry out diverse and specialised functions in distinct tissues. Diversification in tissue function is associated with variation in protein content that is to a large extent determined by patterns of gene expression. One striking example of metabolic compartmentalisation is represented by C_4 photosynthesis where carbon is initially fixed in the mesophyll but is then released and re-fixed in bundle sheath cells. The C_4 pathway is more efficient than C_3 photosynthesis under warm, dry conditions, and as a consequence it has been proposed that engineering the C_4 pathway into C_3 crops such as rice could lead to increased yields[1,2]. Understanding mechanisms directing expression to bundle sheath or mesophyll cells is crucial to this effort and previous work has shown that multiple mechanisms can drive cell type-preferential expression in C_4 species[3]. For example, expression of the *Glycine decarboxylase P subunit (GLDPA)* in the bundle sheath and veins of C_4 *Flaveria bidentis* is due to interplay between multiple regulatory regions[4]. Sequence in the distal promoter generates strong expression but is not tissue-specific, however in the presence of proximal promoter elements, expression in the bundle sheath is brought about by transcripts derived from the distal promoter being degraded in mesophyll cells through nonsense-mediated RNA decay of incompletely spliced transcripts[4,5]. Similarly, for the *Phosphoenolpyruvate carboxylaseA1 (PpcA1)* gene from C_4 *Flaveria trinervia*, two submodules in a distal region that are enhanced by interaction with sequence in the proximal promoter are sufficient to confer mesophyll specificity[6,7]. In addition to promoter sequences, other genic regions contain *cis*-elements that generate tissue-specific gene expression. For example, preferential expression of the *CARBONIC ANHYDRASE2, CARBONIC ANHYDRASE4* and *PYRUVATE,ORTHOPHOSPHATE DIKINASE* genes in mesophyll cells of the C_4 species *Gynandropsis gynandra* is mediated by a nine base pair motif present in both 5' and 3' untranslated regions[8]. Moreover, preferential expression of *NAD-ME1&2* genes in the bundle sheath of *G. gynandra* is associated with two motifs known as Bundle Sheath Modules (BSM) 1a and 1b that co-operatively restrict gene expression to this tissue. BSM1a and BSM1b represent duons because they are located in coding sequence and so determine amino acid composition as well as gene expression[9,10]. In summary, tissue-specific expression can be generated through multiple mechanisms, but factors in *trans* that interact with the *cis*-elements controlling tissue specific patterning of gene expression have not yet been identified.

As the C_4 pathway appears to have evolved repeatedly from the ancestral C_3 state by co-opting existing molecular mechanisms from C_3 leaves[11,12,13] we sought to leverage the C_3

model *Arabidopsis thaliana* (hereafter Arabidopsis) to better understand mechanisms allowing cell type-specific gene expression. The bundle sheath represents about 15% of cells in leaves of Arabidopsis[14] and has been proposed to play important roles in hydraulic conductance[15], transport of metabolites[16], as well as storage of carbohydrates[17], ions[18] and water[19,20]. A number of findings are consistent with bundle sheath cells also being involved in sulphur metabolism and glucosinolate biosynthesis. First, the promoter of *SULPHUR TRANSPORTER2.2* generates preferential expression in the bundle sheath[21,22] and secondly, compared with the whole leaf, transcripts encoding enzymes of sulphur metabolism are more abundant on bundle sheath ribosomes[23]. Transcripts of *MYB76* and other MYB domain transcription factors involved in glucosinolate biosynthesis are also preferentially associated with bundle sheath ribosomes[23] but how this patterning of gene expression is achieved is not known.

To better understand the regulation of cell type-specific gene expression in Arabidopsis we focussed on the *MYB76* gene that is preferentially expressed in the bundle sheath. A classical truncation analysis was combined with computational interrogation of transcription factor binding sites to identify a 256-nucleotide region necessary and sufficient for expression in the Arabidopsis bundle sheath. Within this region we identified MYC and MYB transcription factor binding sites. We show MYC and MYB transcription factors are necessary for *MYB76* expression as well as the expression of at least forty-seven additional genes that are preferentially expressed in the bundle sheath. We propose that the MYC-MYB module previously associated with expression of glucosinolate biosynthetic genes[24] acts as a driver of bundle sheath preferential expression in Arabidopsis. To our knowledge, this work provides the first example of a regulatory system governing the spatial control of gene expression in leaves.

Results

Gene Ontology (GO) analysis of publicly available data[23] indicated that in addition to transcripts encoding proteins important for amino acid export, those encoding glucosinolate (GLS) biosynthesis proteins are strongly enriched in the bundle sheath of Arabidopsis (Figure 1a). In fact, all but five of the thirty genes reported to be involved in GLS biosynthesis[25] showed more than two-fold higher expression in the bundle sheath compared with the whole leaf (Figure 1b). The expression of genes involved in aliphatic GLS metabolism is mostly controlled by MYC and MYB transcription factors[24,26] including MYC2, MYC3, MYC4 and MYB28, MYB29 and MYB76. Notably, genes encoding MYB28, MYB29 and MYB76 were strongly expressed in the bundle sheath compared with the whole leaf (Figure 1b). We sought to use these transcription factors to better understand how gene expression is restricted to the bundle sheath of C_3 plants.

To test whether regions upstream of *MYB28, MYB29* and *MYB76* were sufficient to drive expression in the bundle sheath of Arabidopsis, each was fused to the *uidA* reporter gene encoding GUS and multiple transgenic lines were generated. We were unable to detect GUS staining in leaves from the promoter of *MYB28* alone (Supplementary Figure 1) and whilst the promoter of *MYB29* did mark veins and bundle sheath cells, it also led to some GUS accumulating in mesophyll cells (Supplementary Figure 1). In contrast, a construct containing the promoter and 279bp after the translational start site of *MYB76* generated clearly detectable GUS in the Arabidopsis bundle sheath with no GUS detected in the mesophyll (Figure 1c, Supplementary Figure 2). We conclude that regulatory elements sufficient for bundle sheath expression of *MYB76* (Figure 1b) are contained in this sequence but the preferential accumulation of transcripts from *MYB28* and *MYB29* (Supplementary Figure 1) is likely mediated by *cis*-elements located outside of the sequence tested.

As expression patterns can be determined by *cis*-elements in promoters, untranslated regions, exons, introns or downstream 3' regions[8,9,12,27,28] a translational fusion between the *MYB76* genomic sequence and *uidA* driven by the *MYB76* promoter was generated to confirm that the strong expression in the bundle sheath mediated by the *MYB76* promoter reflected the pattern of expression associated with the intact genomic sequence. Transgenic lines harbouring this genomic fusion showed preferential accumulation of GUS in the bundle sheath (Figure 1d, Supplementary Figure 3) mirroring the pattern found from the promoter alone. Use of the fluorometric 4-MethylUmbelliferyl β-D-Glucuronide (MUG) assay showed that GUS accumulation was lower when nucleotides +280 to +1254 relative to the translational start site were included (Supplementary Figure 6) suggesting that the full genomic sequence of *MYB76* contains regulators that quantitatively repress expression. To

confirm that the GUS reporter generated a reliable read-out of spatial expression patterns, a nuclear localised *pMYB76::H2B::GFP* line was produced. Imaging of GFP in deep tissue of leaves such as the bundle sheath is challenging, but consistent with data from the GUS reporter (Figure 1c), GFP was detectable in nuclei of the vasculature and bundle sheath cells but was absent from the mesophyll (Figure 1e, Supplementary Figure 4). These results show that the promoter of *MYB76* generates bundle sheath preferential expression.

To further investigate the elements driving *MYB76* expression in the bundle sheath, 5' deletions of the promoter were generated. Removal of nucleotides -1725 to -1264 relative to the translational start site did not impact on GUS localisation, however once nucleotides -1264 to -796 were removed GUS was no longer detectable in the bundle sheath. Further removal of another 500 base pairs had no additional impact on the spatial pattern of GUS accumulation (Fig 1f, Supplementary Figure 5). These findings are supported by quantification *via* MUG assays (Supplementary Figure 6) that showed removal of nucleotides -1725 to -1264 reduced accumulation of the reporter, and MUG was no longer detectable once sequence upstream of nucleotide -796 was absent. Overall, these data indicate that the *MYB76* promoter contains a region between nucleotides -1264 and -796 upstream of the translational start site that directs expression to the bundle sheath.

A DHS necessary and sufficient for bundle sheath expression

The DNaseI enzyme preferentially cuts accessible DNA and so can be used to define sequences available for transcription factor binding and thus the location of regulatory DNA[29]. To complement our truncation analysis, an existing dataset that defined DNaseI Hypersensitive Sites (DHS) in Arabidopsis[30] was interrogated. Two DHS were detected upstream of *MYB76* in both flower tissue and leaves (Figure 2a) with a DHS encompassing nucleotides -909 to -654 upstream of the translational start site overlapping with the region required for expression in the bundle sheath (Figure 1f). Consistent with the DHS data, *MYB76* has been reported to be expressed in both leaves and flowers[26]. Although the DHS had a lower DHS score in the leaf than the flower (mean DHS score of 1.3 versus 2.6[31]), this may be due to the fact that bundle sheath cells make up a small proportion of cells in a C_3 leaf[14] such that transcription factor binding upstream of *MYB76* would be diluted in whole leaves.

Removing the DHS found between nucleotides -909 to -654 of the *MYB76* promoter abolished accumulation of GUS, and fusing this DHS to the minimal *CaMV35S* promoter was sufficient to generate GUS in the bundle sheath (Figure 2b, Supplementary Figure 7). Furthermore, oligomerizing two copies of the DHS upstream of the minimal *CaMV35S*

promoter resulted in very strong accumulation of GUS in the bundle sheath (Figure 2b, Supplementary Figure 7). From these data we conclude that sequence within this DHS is both necessary and sufficient to activate expression preferentially in the bundle sheath. Combined with the truncation analysis indicating that nucleotides -1264 to -796 upstream of the translational start site were required for expression in the bundle sheath (Figure 1f, Supplementary Figure 5), our findings indicate that a positive regulator of bundle sheath expression is located between nucleotides -909 (the start of the DHS) and -796 upstream of the *MYB76* translational start site.

Phylogenetic foot-printing identified two motifs (Figure 2c) in the *MYB76* DHS that are shared by *MYB76* and the promoters of *SCR, SULTR2.2* and *GLDP* that have previously been reported to generate expression in the Arabidopsis bundle sheath[5,21,22,32]. Whilst site directed mutagenesis of motif one (TGGGCA) had no impact on accumulation of GUS in the bundle sheath (Supplementary Figure 8) deletion of motif two (TGCACCG) in the context of the full genomic sequence of *MYB76* abolished GUS accumulation in the bundle sheath (Figure 2d, Supplementary Figure 9). These data indicate that this sequence is necessary to pattern expression from both the promoter of *MYB76* alone, but also the full genic *MYB76* sequence containing exons, introns and UTRs. To test whether this sequence is sufficient to direct expression to the bundle sheath it was combined with ten upstream and ten downstream nucleotides from the endogenous *MYB76* promoter, oligomerized, and fused to *uidA*. Although this construct did not recapitulate the strong bundle sheath expression of the *MYB76* DHS it was able to generate weak expression in the bundle sheath (Figure 2d, Supplementary Figure 10). We conclude that the 27bp sequence is necessary and weakly sufficient to direct expression to the bundle sheath.

MYC, MYB and DREBs control bundle sheath expression

To better understand the *cis*-regulatory landscape within the *MYB76* DHS we used the Find Individual Motif Occurrences (FIMO) tool[33] to predict transcription factor binding sites. For the majority of Arabidopsis transcription factors, DNA binding sites have not yet been defined, and so to allow us to search for broad consensus sequences associated with groups of transcription factors we clustered the 555 transcription factor binding motifs for Arabidopsis from the JASPAR motif database[34] into 43 groups based on relatedness of the motif position weight matrices (PWMs) (Supplementary Table 1). Plotting matches for each of these motifs in the *MYB76* DHS (Figure 3a) showed that it contained binding sites for motifs from twelve clusters. Notably the 27bp region necessary for expression in the bundle sheath contained binding sites from clusters 1, 8, 11 and 16 that correspond to the binding

sites from ERF (clusters 1 and 11), bHLH (cluster 8), and G2-like (cluster 16) transcription factor families. There are also predicted binding sites for IDD (cluster 9), MADS (cluster 23) and MYB (clusters 10 and 18) families within the DHS. To supplement this *in silico* analysis, Yeast One-Hybrid identified thirteen transcription factors from seven different families that were able to bind the DHS (Figure 3b). Six of these transcription factors including DF1, MYB73 and AIL5 were previously reported to bind the whole *MYB76* promoter[25] (Figure 3b). Although not identified by Yeast One-Hybrid, MYC2, MYC3, MYC4, MYB28 and MYB29 can control *MYB76* expression[24,26] and so were incorporated into our list of candidate regulators of *MYB76*. Of these candidates, *MYB28*, *MYB29*, *DF1*, *MYB73* and *AIL5* were strongly preferentially expressed in the bundle sheath (with a log2(bundle sheath/whole leaf) > 0.75 cut off) (Figure 3b).

We next tested whether these candidate transcription factors could activate expression from the *MYB76* DHS *in planta.* For the following reasons we chose to test MYC2, MYC3, MYC4, DREB2A, DREB26, DF1 and MYB73. First, MYC2, MYC3, MYC4, DREB2A and DREB26 have binding sites for the clusters described above within the 27bp region and MYC2, MYC3 and MYC4 have previously been reported to affect *MYB76* expression[24]. Second, DREB2A was found in our Yeast One-Hybrid experiment and DREB26 was identified in both Yeast One-Hybrid screens (Figure 3b). Third, DF1 and MYB73 were found in both Yeast One-Hybrid studies (Figure 3b), are preferentially expressed in the bundle sheath (Figure 3b) and DF1 has previously been associated with *GLS* gene expression[25]. Although the DHS contains two additional predicted MYB binding sites (one associated with cluster 10 and one with cluster 18 MYBs) these were outside the region necessary for activating *MYB76* expression in the bundle sheath (Figure 3a). Each transcription factor was used in a *trans*-activation assay for the *MYB76* DHS in *Nicotiana benthamiana.* Infiltration with MYC2, MYC3, MYC4 and DREB2A resulted in significantly more LUCIFERASE (LUC) signal than infiltration with the DHS alone, with MYC2, MYC3 and MYC4 driving higher LUC signal than DREB2A (Figure 3c). LUC signal was not significantly different from the DHS alone for any of the other transcription factors tested (Figure 3c).

As the MYCs (Cluster 8) and DREB2A (Cluster 11) have predicted binding sites that overlap the 27bp region necessary for expression in the bundle sheath (Figure 2c and Figure 3a) and were able to activate expression from the DHS in the *trans*-activation assays (Figure 3c) we tested whether expression of *MYB76* was perturbed in mutant alleles of each. qRT-PCR on *MYB76* was performed on *myc2/3/4* and *dreb2a* mutants. *MYB76* expression was reduced by approximately half in the *dreb2a* mutant, and in the *myc2/3/4* triple mutant by about 19 times (Figure 3d). These data are consistent with the *trans*-activation results which

showed a strong increase in expression driven by MYC transcription factors and a weaker increase driven by DREB2A (Figure 3c). Taken together this indicates that under the conditions we used MYC2, MYC3 and MYC4 have a major role in controlling *MYB76* expression and DREB2A has a smaller effect. Previous work has shown that MYC transcription factors interact with MYB28, MYB29 and MYB76 to activate the expression of genes involved in GLS metabolism[24]. Therefore, despite them not appearing in either Yeast One-Hybrid screen, we asked whether they are involved in controlling *MYB76* expression. Re-analysis of publicly available data[35] showed that *MYB76* expression was substantially reduced in a *myb28/29* mutant (Figure 3e). This is consistent with previous reports of MYB28, 29 and 76 being able to activate each other's expression[26]. *MYB76* is expressed at similar levels to wild type in both *myb28* and *myb29* single mutants[36] suggesting that there is redundancy between *MYB28* and *MYB29* in the control of *MYB76* expression. Although *MYB29* and *MYB76* are tandem duplicates on chromosome five, because *MYB76* is expressed similarly to wild type in a *myb29* mutant, the reduction of *MYB76* expression in the *myb28/29* mutant is unlikely to be a result of the proximity of the *myb29-1* T-DNA insertion to *MYB76.* MYB28, 29 and 76 do not have defined transcription factor binding motifs in publicly available databases, however mapping motif clusters to a phylogenetic reconstruction of MYB transcription factors (Supplementary Figure 11) showed that MYB28, MYB29 and MYB76 were found in the cluster 18 clade, strongly suggesting that their binding preference is similar to those of the cluster 18 MYBs with transcription factor binding motifs found in the *MYB76* DHS (Supplementary Figure 12). Although we do not show direct regulation of *MYB76* by MYB28 and MYB29 from the DHS, the data presented, combined with that from previous studies[24,26], are consistent with a model where *MYB76* expression is controlled by MYC and MYB transcription factors activating *MYB76* from the DHS (Figure 3f and Figure 3g).

MYC2/3/4 and MYB28/29 control other bundle sheath genes

The findings above are consistent with the MYC-MYB module, previously reported to activate GLS metabolism genes in response to herbivory[24] (Figure 3f and Figure 3g) activating *MYB76* in the bundle sheath in the absence of herbivory. As this module is involved in activating the expression of multiple GLS metabolism genes in Arabidopsis[24] and most are preferentially expressed in the bundle sheath (Figure 1b), we wished to test whether the MYC-MYB system might also be responsible for their bundle sheath preferential expression. We therefore re-analysed publicly available transcriptome data for *myc2/3/4*[37] and *myb28/29*[35] mutants. We identified 207 genes that were down-regulated (log2 vs. WT

< -0.75) in *myc2/3/4* (Figure 4a), 729 genes that were down-regulated in *myb28/29* (Figure 4b) and 76 genes that were down-regulated in both *myc2/3/4* and *myb28/29* (Figure 4c). Next, we used a published dataset[23] to test whether any of these gene sets were preferentially associated with the Arabidopsis bundle sheath. Genes down-regulated only in *myc2/3/4* (Figure 4d) or *myb28/*29 (Figure 4e) were not preferentially expressed in either the bundle sheath or whole leaf. However, of the 54 genes down-regulated in both *myc2/3/4* and *myb28/29* and present in the cell-type specific translatome dataset[23], 47 were strongly bundle sheath preferential (log2(bundle sheath/whole leaf) > 0.7) (Figure 4f). Only four genes were strongly depleted in the bundle sheath (log2(bundle sheath/whole leaf) < -0.7) (Figure 4f). Consistent with these down-regulated genes being directly regulated by the MYC-MYB system, motif enrichment analysis showed that the MYC2/MYC3/MYC4 (cluster 8) and MYB28/MYB29 (cluster 18) motifs were strongly enriched in promoters of genes down-regulated in both *myc2/3/4* and *myb28/29* mutants (Figure 4i). This was not the case for the *myc2/3/4* mutant (Figure 4g) or the *myb28/29* mutant alone (Figure 4h).

Previous work suggested that MYBs and MYCs bind to adjacent regions of promoters to activate expression of *GLS* genes[24] (Figure 3f). This was also the case in the *MYB76* DHS (Figure 3a). To test if this was also true for genes down-regulated in both *myc2/3/4* and *myb28/29* we investigated minimum distance between cluster 8 and 18 motifs in each set of promoters and compared this with random sets of genes. This showed that as well as being more enriched in the promoters of down-regulated genes in both mutants (Figure 4i) where cluster 8 and 18 motifs were both present, they were closer together in the down-regulated genes common to *myc2/3/4* and *myb28/29* compared with those down-regulated in only one mutant background, or in any of the random sets (Figure 4j). In summary, genes down-regulated in both *myc2/3/4* and *myb28/29* were generally strongly preferential to the bundle sheath, showed an enrichment of MYC2/3/4 and MYB28/29/76 binding sites in their promoters and where these motifs are both present, they were closer together than the other gene sets that we assessed. Taken together these findings suggest that the MYC-MYB module is important in controlling the expression of at least forty-seven genes in the bundle sheath of Arabidopsis.

Discussion

Although many promoters allowing expression in defined tissues of the shoot or root have been reported, our understanding of how these expression domains are generated is limited. Examples include promoters that drive expression in tissues such as apical meristems[38,29,40,41,42] the stele[43,44], endodermis[32], cortex[45,46] and trichoblasts or atrichoblasts[47,48] of the root, as well as guard cells[49], phloem companion cells[50] and epidermal cells[51] of the shoot. In leaves, perhaps the best characterised of these promoters come from analysis of C_4 species[4,6,7]. For example, mesophyll specific expression of *PPCA1* from *F. trinervia* is due to two modules in a distal region of the promoter[6,7] whilst the *GLDPA* promoter from C_4 *F. bidentis* generates expression in the bundle sheath because proximal promoter sequence leads to transcripts derived from a distal promoter element being degraded in mesophyll cells[4,5]. In roots, using *SHORTROOT* as a model, it has been proposed that multiple *cis*-elements recognised by a complex network of both activators and repressors confine expression to the root vasculature[52]. Analysis of transcription factor binding *in vivo* is consistent with a highly combinatorial mosaic of regulatory DNA underpinning patterns of gene expression[53]. To our knowledge, and perhaps due to this highly complex regulatory landscape, there are no examples of *cis*-elements and interacting transcription factors that limit gene expression to specific cell types in leaves. In this work, we show that combining DNaseI-SEQ data with functional analysis allowed identification of *cis*-elements and cognate transcription factors that pattern expression to bundle sheath cells of the leaf.

The module that generates expression in bundle sheath cells contains two *cis*-elements recognised by MYC and MYB transcription factors. When sequence containing this region is oligomerised it leads to strong and specific expression in the bundle sheath and so represents a short sequence that could be used to mis-express genes in this tissue. Bundle sheath cells link the vasculature to the photosynthetic mesophyll cells. In C_3 species, they play important roles including the control of hydraulic conductance[15,19,20] transport of metabolites in and out of veins[16], responses to high light episodes[54], and assimilation of sulphur[23]. However, there are relatively few promoters available to drive or perturb expression in these cells[21,32]. Short synthetic promoters have a number of advantages over the long promoter fragments currently available to direct gene expression to bundle sheath cells. These include reducing the likelihood of homology-based gene silencing if used more than once in any construct[55] and decreasing the chances of leakiness or off-target gene expression associated with use of full-length promoter fragments[56]. Oligomerization of *cis*-elements to achieve higher expression levels is a common strategy when creating synthetic

promoters[57]. As the *MYB76* DHS is short and can be oligomerized to tune expression levels, it appears to represent a promising fragment with which to perturb and modify functions including the control of hydraulic conductance, metabolite transport, responses to high light, and assimilation of sulphur in the bundle sheath.

Control of bundle sheath expression by a MYC-MYB module

Glucosinolates are a diverse group of nitrogen and sulphur containing secondary metabolites that accumulate preferentially around the mid-vein and outer lamina in Arabidopsis rosette leaves and which are involved in defence against herbivory[58]. The methionine-derived aliphatic glucosinolate biosynthetic pathway is largely controlled by MYB28, MYB29 and MYB76 in combination with MYC2, MYC3 and MYC4[24,25,26,36,59,60] (Figure 3f). The *MYB76* promoter has previously been reported to generate expression in the vasculature[26]. Our analysis now shows that its expression domain includes the bundle sheath, and that this is under control of a MYC-MYB module (Figure 3g). None of the MYC2*,* MYC3*,* MYC4*,* MYB28*,* MYB29 or MYB76 transcription factors were identified in our Yeast One-Hybrid analysis (Figure 3b) or previously published analysis of the whole *MYB76* promoter[25]. This may be due to these transcription factors requiring additional partners to bind DNA, consistent with the model of MYC-MYB dimers being required for the activation of target genes[24]. Although this appears inconsistent with the *trans*-activation assays where infiltration of individual MYC transcription factors activated expression from the *MYB76* DHS (Figure 3c), this may be due to their interaction with endogenous MYBs from *N. benthamiana*. Alternatively, and consistent with the MYC binding site alone being able to generate weak expression in the bundle sheath (Figure 2d), the interaction may be below the detection limit of the Yeast One-Hybrid assay.

It is theoretically possible that this MYC-MYB module acts as a general activator of transcription across all cells of the leaf and another distinct mechanism represses expression in other cell types. However, for the following reasons, we favour a model in which the MYC-MYB module activates expression preferentially in the bundle sheath. First, the 256bp DHS which contains the MYC-MYB binding sites is sufficient for bundle sheath preferential expression, and the 27bp region containing the potential MYC binding site (Figure 2c) but lacking MYB binding sites, is sufficient for weak expression in the bundle sheath (Figure 2d). Second, *MYB28* and *MYB29* are preferentially expressed in the bundle sheath (Figure 1b) consistent with them activating expression in this cell-type. Third, other transcription factor binding sites required for directing bundle sheath preferential expression would have to be present in the 27bp region. This is possible, however we would expect

such binding sites to be enriched in promoters of additional genes that are strongly expressed in the bundle sheath of wild-type plants but down regulated in both *myc2/3/4* and *myb28/29* mutants. No such binding sites were detected (Figure 4i). In summary, we cannot completely rule out a requirement for other factors operating in other cell types such that *MYB76* expression is restricted to the bundle sheath. However, the MYC-MYB module activating expression preferentially in the bundle sheath is a more parsimonious mechanism. To our knowledge, this MYC-MYB module provides the first example of a regulatory system governing the spatial control of gene expression in leaves.

At this point, how the MYC-MYB module directs preferential expression in the bundle sheath is not clear. *MYB28* and *29* transcripts accumulate preferentially in the bundle sheath (Figure 1b) but this is not as apparent for transcripts of genes encoding *MYC2, MYC3* and *MYC4* (Figure 3b). MYC transcription factors are regulated by jasmonic acid (JA) signalling thorough interactions with JASMONATE-ZIM DOMAIN (JAZ) proteins[61,62]. Whether there is a link between JA signalling and bundle sheath preferential gene expression remains to be determined.

Roles of additional transcription factors in controlling *MYB76*

Many additional transcription factors were identified as binding the *MYB76* DHS in Yeast One-Hybrid analysis (Figure 3b) and some of these have been reported to bind the entire promoter previously[25]. These transcription factors are likely important for controlling other aspects of *MYB76* expression in addition to the spatial patterning determined by the MYC-MYB module. For example, multiple ERF family transcription factors interacted with the *MYB76* DHS (Figure 3b) and there is an ERF family transcription factor binding site in the DHS (Figure 3a). Additionally, DREB2A weakly activates expression from the *MYB76* DHS (Figure 3c) and *MYB76* transcripts were less abundant in a *dreb2a* mutant allele (Figure 3d). Recent work has linked auxin signalling and glucosinolate biosynthesis under drought conditions with DREB2A/B signalling[63]. This suggests that DREB2A may have a role in regulating *MYB76* expression in response to environmental stimuli. Because DREB2A transcripts do not accumulate preferentially in the bundle sheath (Figure 3b) it is not clear how activation of *MYB76* outside of the bundle sheath is avoided. Possibilities include DREB2A activity being limited to the bundle sheath by post-transcriptional and/or post-translational mechanisms or a requirement for other binding partners. Post-transcriptional and post-translational regulation has been reported for DREB2A[64] with post-transcriptional regulation by alternative splicing being reported[65,66,67,68]. Whilst overexpression of *DREB2A* in Arabidopsis does not affect the expression of target genes[69] an isoform lacking key

phosphorylation sites activates the majority of DREB2A targets[70]. Thus, post-translational regulation is essential for DREB2A activity suggesting a mechanism for restricting DREB2A activation of *MYB76* expression to the bundle sheath. The *MYB76* DHS also contains a MADS domain transcription factor binding site (Figure 3a). MADS domain transcription factors are involved in controlling gene expression required for flower development[71] and could potentially be involved in directing *MYB76* expression to flowers where significant levels of GLS accumulate[72]. In summary, as well as the MYC-MYB module generating bundle sheath preferential expression in leaves, multiple other transcription factor binding sites in the DHS may be important for controlling other aspects of *MYB76* expression such as responses to environmental stimuli and expression in different organs.

The MYC-MYB module outside glucosinolate biosynthesis

Our data are consistent with the MYC-MYB module patterning the expression of at least forty-seven genes to the Arabidopsis bundle sheath. This represents about 3.6% of the 1316 genes previously reported to be preferentially expressed in the bundle sheath (using a log2(bundle sheath/whole leaf) cut off >1)[23] indicating that this module must operate alongside other networks. This notion is supported by previous analysis of promoters controlling bundle sheath preferential expression in Arabidopsis. For example, the region identified as controlling the bundle sheath preferential expression of *SULTR2;2*[22] does not contain the MYC-MYB module.

Although extensive glucosinolate biosynthesis is confined to the Brassicaceae[73] there are indications that this MYC-MYB module patterns genes unrelated to glucosinolates to the bundle sheath. One possibility is associated with glucosinolate biosynthesis representing a derived pathway that has evolved in the Brassicaceae. It would seem more parsimonious if its patterning to bundle sheath cells was mediated by integration into an existing gene regulatory network associated with this cell type, than through evolution of a network *de novo*. This seems plausible because in addition to several enzymes of primary sulphur metabolism being part of the core glucosinolate biosynthesis pathway[74], transcripts encoding many enzymes of sulphur transport and assimilation are more abundant in the bundle sheath compared with whole leaves[23]. This raises the possibility that compartmentation of glucosinolate biosynthesis to the bundle sheath may have occurred through acquisition of *cis*-elements that restrict the expression of sulphur assimilation genes to this cell-type. In Arabidopsis the MYC-MYB protein-protein interaction is mediated by a MYC-Interaction-Motif (MIM) that is only found in MYBs involved in aliphatic (MYB28, MYB29 and MYB76) and indolic (MYB34, MYB51 and MYB122) glucosinolate metabolism,

as well as the more distantly related MYB47 and MYB95[75]. This is consistent with the proposed roles of MYB28 and MYB29 as part of a MYC-MYB module controlling bundle sheath expression in Arabidopsis. The MIM is a short linear motif found in intrinsically disordered regions of MYB proteins and as such has been suggested to have the potential to evolve rapidly[75]. It is therefore possible that the control of bundle sheath preferential expression by a MYC-MYB module in other species is mediated by MYBs that are more distantly related to MYB28 and MYB29 that have acquired a MIM and therefore the ability to interact with MYC transcription factors.

In addition to genes associated with sulphur metabolism, there is also evidence that this MYC-MYB module may pattern genes that are thought to represent some of the first steps towards evolving C_4 photosynthesis. Although the Arabidopsis *GLYCINE DECARBOXYLASE P-PROTEIN 1 (GLDP1*) gene is expressed strongly in both the mesophyll cells and the vasculature, deletion of an M-box in the promoter resulted in bundle sheath expression of *GLDP1*[76]. The remnant expression in the bundle sheath and vein tissue was associated with a 266bp region named the V-box[76]. Re-analysis of these 266bp identified MYC and MYB binding sites within 25bp of each other (Supplementary Figure 12). It is possible that constitutive expression of *GLDP1* in the C_3 Arabidopsis leaf is due to the M-box and MYC-MYB modules driving expression in mesophyll and bundle sheath strands respectively. This is consistent with the MYC-MYB module being an activator of expression in the bundle sheath and therefore its presence not preventing activation in other cell types. This would explain why only some genes containing the MYC-MYB module are preferentially expressed in bundle sheath strands and suggests that bundle sheath preferential expression is partly defined by lack of activation in other cell-types.

One of the early events associated with the transition from C_3 to C_4 photosynthesis is thought to be the restriction of the Glycine Decarboxylase complex to the bundle sheath as part of establishing a C_2 photosynthetic cycle[77]. The M-box of *GLDP1* is highly conserved in the Brassicaceae, but is lost in *Moricandia nitens*, a species that uses C_2 photosynthesis and partitions *GLDP* to bundle sheath cells. Conversely the V-box, and predicted MYC and MYB binding sites, is conserved in *M. nitens*[76,78]. It is therefore possible that during the evolution of C_2 photosynthesis in the Brassicaceae, the MYC-MYB module in *GLDP* is responsible for bundle sheath expression of the *GLDP* gene once the M-box is lost.

In summary we report a MYC-MYB module that directs gene expression to the bundle sheath of Arabidopsis. To our knowledge, this provides the first example of a regulatory system governing the spatial control of gene expression in leaves. In the future it will be

interesting to determine if this module has been co-opted during the evolution of C_4 photosynthesis to pattern components of the C_4 cycle to this cell type.

Materials and methods

Plant material, growth conditions and cloning

Seed of Arabidopsis was sterilised by washing in 70% (v/v) ethanol for 3 minutes followed by washing in 100% ethanol for 1 minute. Transformants were selected on 0.5% (w/v) Murashige & Skoog medium (pH 5.8) 1% (w/v) agar with the relevant antibiotics. After 2-3 days of stratification in the dark at 4°C, tissue culture plates were transferred to a 16 hour photoperiod growth chamber with a light intensity of 200 µmol m^{-2} s^{-1} photon flux density, 65% relative humidity and a temperature cycle of 24°C (day) and 20°C (night). Transformed seedlings were transferred onto 3:1 Levington M3 high nutrient compost and Sinclair fine Vermiculite soil mixture and grown for another 2-3 weeks before analysis. *N. benthamiana* plants used for transient assays were grown from seed in pots containing the same soil mixture with a 16 hour photoperiod, 200 µmol m^{-2} s^{-1} photon flux density, 60% relative humidity and 22°C.

T-DNA insertion mutants for *dreb2a* (GK-179C04) were obtained from the Nottingham Arabidopsis Stock Centre (NASC). T-DNA insertion lines were genotyped to identify lines homozygous for the required T-DNA insertion and RT-PCR was performed to confirm that the mutation resulted in the loss of *DREB2A* gene expression.

The full length *MYB76* gene as well as the promoter alone were amplified from Arabidopsis *Col-0* genomic DNA and then fused to *uidA*. The minimal CaMV35S promoter was synthesised and fused to *MYB76 DH*S by polymerase chain reactions (PCR). Deletion of the DHS within the promoter was achieved by PCR fusion of the 5' end of the promoter with the 3' end of the promoter prior to being cloned into the pENTR/D TOPO vector. Each forward primer contained a CACC overhang to ensure directional cloning. A Gateway LR reaction was performed to transfer the relevant inserts into a modified pGWB3 vector[79] that contained an intron within the *uidA* sequence. To generate constructs for GFP imaging *pMYB76* and *2xDHS_CaMV35SMin* fragments in a pENTR vector were cloned using a Gateway LR reaction into a modified pGWB1 vector containing a *H2B::GFP* fusion. *MYB76gDNA::uidA*, *2xDHS_CaMV35SMin::uidA* and *2x27_CaMV35SMin::uidA* were constructed using Golden Gate technology[80]. Motif substitutions were made using the QuikChange Lightning Site-Directed Mutagenesis (Agilent Technologies) and motif deletions were made by overlapping PCR. Constructs were then placed into *Agrobacterium tumefaciens* strain GV3101 and introduced into Arabidopsis Col-0 by floral dipping[81].

Constructs for *trans*-activation assays were made using the Golden Gate system. Coding sequence of candidate transcription factors were cloned from Arabidopsis cDNA, domesticated to remove *Bpi*I and *Bsa*I restriction sites and cloned into level 0 vectors. Level

1 constructs were generated to constitutively express candidate transcription factors, to constitutively express a p19 silencing suppressor, to constitutively express a GUS reporter to act as an infiltration control and to fuse the *MYB76* DHS with a *LUCIFERASE* reporter to provide an output of activation from the DHS. These level 1 constructs were then assembled into level 2 modules and transformed into *A. tumefaciens* GV3101. Constructs for the constitutively active LjUBI promoter, the OCS1 terminator, LUC coding region, GUS coding region have been published previously[82] and parts were cloned into appropriate Golden Gate vectors[83].

GUS staining, MUG assays, and GFP imaging

To take into account position effects associated with transgene insertion site, GUS staining was undertaken on at least six randomly selected T1 plants for each *uidA* fusion[84]. The staining solution contained 0.1 M Na_2HPO_4 pH 7.0, 2 mM potassium ferricyanide, 2 mM potassium ferrocyanide, 10 mM EDTA pH 8.0, 0.06% (v/v) Triton X-100 and 0.5 mg ml^{-1} X-gluc. Leaves from three-week old plants were vacuum-infiltrated three times in GUS solution for one minute and then incubated at 37°C for between 3 and 72 hrs depending on the strength of the promoter being assessed. Next, stained samples were fixed in 3:1 (v/v) ethanol:acetic acid for 30 minutes at room temperature, cleared in 70% (v/v) ethanol at 37°C and then placed in 5 M NaOH for 2 hrs. Samples were stored in 70% (v/v) ethanol at 4°C. Samples were imaged with an Olympus BX41 light microscope with Q Capture Pro 7 software and a QImaging MicroPublisher 3.3 RTV camera. To quantify reporter accumulation from each promoter the quantitative assay that assesses the rate of MUG conversion to 4-methylumbelliferone (MU) was performed on between 10 and 25 lines[84]. Tissue was frozen in liquid nitrogen, homogenised and soluble protein extracted in 5 volumes of Protein extraction buffer (1 mM $MgCl_2$, 100 mM NaCl, 50 mM Tris (Melford) pH7.8). 15 µl of protein extract was incubated with 60 µl of MUG at 37 ºC for one, two, three and four hours respectively. The reaction was stopped after each time point by addition of 75 µl 200 mM anhydrous sodium carbonate. GUS activity was analysed via measurements of fluorescence of MU at 455 nm after excitation at 365 nm. The concentration of MU/unit fluorescence in each sample was interpolated using a concentration gradient of MU over a linear range.

GFP imaging was performed on at least seven independent T1 lines of *pMYB76::H2B::GFP* and *2xMYB76_DHS::H2B::GFP.* Rosette leaves of four week old plants were sampled and outer tissue layers were removed by scraping leaves with a razor blade under 1X PBS solution. Samples were imaged on a Leica TCS SP8 confocal microscope,

GFP was excited at 488 nm and emission was detected at 500-530 nm. Images were recorded on LAS Image analysis software (Leica) and processed to merge channels and add scale bars in ImageJ v1.52a (https://imagej.nih.gov/ij/).

Yeast One-Hybrid screen

Regions screened for transcription factor binding via Yeast One-Hybrid were first inserted into pENTR 5'TOPO TA entry vector (Thermofisher) and subsequently placed into the pMW2 and pMW3 destination vectors containing *HIS3* and *LACZ* marker genes respectively[85]. The enhanced Yeast One-Hybrid screen against a complete collection of 2000 Arabidopsis transcription factors was undertaken as described previously[86,87,88]. Details of the bait sequence and list of interactors found in Supplementary Table 4.

***Trans* activation assays and qRT-PCR**

To test interactions between the *MYB76* DHS and transcription factors *in planta* transient infiltration of *N. benthamiana* was performed. Overnight cultures of *A. tumefaciens* were pelleted and re-suspended in infiltration buffer (10mM MES (pH5.6), 10mM $MgCl_2$, 150μM acetosyringone) to an optical density of 0.3. Cultures were then incubated for 2hrs at room temperature and infiltrated into the abaxial side of leaves of four-week old plants with a 1 ml syringe.

Leaf discs from infiltrated regions were sampled 48hrs after infiltration and flash frozen in liquid N_2. Protein for MUG and LUC assays was extracted on ice in 1x passive lysis buffer (PLB: Promega). MUG assays were performed by adding 40μl of protein extract to 100μl of MUG assay buffer (2mM MUG, 50mM Na_3PO_4/Na_2PO_4 buffer (pH 7.0), 10 mM EDTA, 0.1% (v/v) Triton X-1000, 0.1% (w/v) Sodium Lauroyl sarcosinate and 10 mM DTT). Stop buffer (200 mM Na_2CO_3) was added at 0 and 30 mins and rate of MUG accumulation was measured in triplicate on a plate reader (CLARIOstar, BMG lab tech) with excitation at 360 nm and emission at 465 nm. LUC activity was measured with 20 μl of protein sample and 100 μl of LUC assay reagent (Promega). Activation from the DHS was calculated as (LUC luminescence/rate of MUG accumulation) x 100.

Single rosette leaves from four-week old col-0, *dreb2a* and *myc2/3/4* plants were sampled six hours after the onset of light and flash frozen in liquid N_2. RNA was extracted with the RNeasy plant mini-kit (Qiagen) as manufacturer's instructions and cDNA was synthesised using the Superscript double stranded cDNA synthesis kit as manufacturer's instructions (Invitrogen) with on-column DNase1 treatment. qRT-PCR was performed using SYBR green master mix (Bio-Rad) on a CFX384 touch Real-Time PCR Detection System (Bio-RAD).

Transcripts of *MYB76* were normalised to the expression of *ASCORBATE PEROXIDASE 3 (APX3: At4g35000), ASPARTIC PROTEINASE A1 (APA1: At1g11910)* and *UBIQUITIN CONJUGATING ENZYME 21 (UBC21: AT5G25760).* Relative expression was determined using the single delta Ct method and the data reported are from normalisation against *APA1.* Results were very similar regardless of the reference genes used.

Datasets, GO term analysis and *de novo* motif identification

Computational analysis used previously published Arabidopsis datasets for bundle sheath and whole leaf translatomes[23], *myc2/3/4* mutants and col-0[37], and *myb28/29* mutants and col-0[35]. For Gene Ontology (GO) term enrichment analysis the top 200 most bundle sheath preferential (log2(bundle sheath expression/35S expression) genes in the cell-type specific translatome[23] were used as input. The AgriGO tool v2.0[89] was used with default parameters and all genes annotated in the Arabidopsis TAIR10 genome were sued as background. The MEME tool from The Multiple Em for Motif Elucidation (MEME) suite v.4.8.1.[90] was applied to search for conserved motifs within promoter sequences of genes expressed in the Arabidopsis bundle sheath. Maximum length of the motif was set to eight nucleotides, both strands of the sequence were searched and each motif had to be present in every sequence.

To cluster transcription factor binding motifs the RSAT matrix-clustering tool[91] was run on all Arabidopsis motifs from the JASPAR motif database[92] using default parameters which generated 43 motif clusters. The Find Individual Motif Occurances (FIMO)[33] was used to scan DNA sequences for matches to Arabidopsis transcription factor binding motifs found in the JASPAR motif database[92]. To account for input sequence composition a background model was generated using the fasta-get-markov tool from the MEME suite[90]. FIMO was then run with default parameters and a p-value cut-off of 1e-04.

Motif enrichment in promoters of gene sets was analysed using a custom BASH script. Promoter regions (1500bp) were extracted using the getfasta tool from Bedtools[93]. These promoters were scanned for transcription factor binding motifs using FIMO (as above) and counts of motifs in gene sets were recorded. Frequency of a given motif in a gene set was calculated as a proportion of the total motifs and enrichment was calculated as frequency vs background frequency. Background frequency was defined as mean motif frequency in promoters of three random sets of 2000 Arabidopsis genes. Results of motif frequency analysis presented as the log2 of enrichment and motifs sorted by motif cluster. FIMO outputs were sorted to only include matches to cluster 8 and 18 motifs and a custom Python

script was used to find the minimum distance between the centres of cluster 8 and 18 motif in the same promoter.

Statistics and reproducibility

For statistical analysis extreme outliers were identified and removed from analysis. Normality of the data was assessed using the Shapiro-Wilks test. Where data were normally distributed pairwise T-tests were used to assess significance. Where data were not normally distributed, Wilcoxon rank-sum tests were used to assess significance. Levene's test was used to assess equality of variance. Where variance was equal standard deviations were pooled, where variance was not equal variance was not pooled. All tests were two-sided. Pairwise T-tests with pooled SD were used to assess significance in *trans*-activation assays and without pooled SD in qRT-PCR assays. Wilcoxon rank sum tests were used to assess significance for differences in distributions of minimum differences between cluster 8 and 18 motifs in different gene sets. All statistical analysis was performed using R[94] and plots generated using ggplot2 (Wickham, 2009). For GUS staining and GFP imaging, representative images from multiple independent T1 lines are shown. All imaging experiments apart from Supplementary Figure 1 were performed independently on at least two different days with plants grown independently.

Code availability

All code associated with this manuscript is available in the Github repository: https://github.com/hibberd-lab/Dickinson_Knerova_Arabidopsis_bipartite_transcription_factor_module.

Data availability

Underlying data required to generate plots are available in the Github repository: https://github.com/hibberd-lab/Dickinson_Knerova_Arabidopsis_bipartite_transcription_factor_module. Arabidopsis transcription factor motifs downloaded from the JASPAR motif database http://jaspar.genereg.net/. All other data available on request.

Acknowledgements

The work was funded by ERC grant RG80867 Revolution, BBSRC Grants BBP0031171, BB10022431, BB/M011356 to JMH and a Derek Brewer PhD studentship to JK. SMB was

654 partially funded by an HHMI Faculty Scholars fellowship. We thank Roberto Solano
655 (Centro Nacional de Biotecnología, Madrid) for seeds of the *myc2/3/4* triple mutant.
656

657 **Author contributions**

658 PJD, JK, MS, SRS, SJB, HM, A-M B and AG carried out the work. JK, PJD, SMB and JMH
659 designed the work. PJD, JK and JMH wrote the manuscript. JMH initiated and oversaw the
660 project.
661

662 **Competing interests**

663 The authors have no competing interests as defined by Nature Research, or other
664 interests that might be perceived to influence the results and/or discussion reported in this
665 paper.
666

References

1. Hibberd, J.M., Sheehy, J.E. & Langdale, J.A. Using C_4 photosynthesis to increase the yield of rice - rationale and feasibility. *Current Opinion in Plant Biology* **11**, 228–231 (2008).
2. Von Caemmerer, S., Quick, W.P. & Furbank, R.T. The development of C_4 rice: Current progress and future challenges. *Science* **336** 671–1672 (2012).
3. Hibberd, J.M. & Covshoff, S. The Regulation of Gene Expression Required for C_4 Photosynthesis. *Annu. Rev. Plant Biol* **61**, 181–207 (2010).
4. Wiludda, C. et al. Regulation of the photorespiratory *GLDPA* gene in C_4 *Flaveria*: an intricate interplay of transcriptional and posttranscriptional processes. *Plant Cell* **24**, 137–151 (2012).
5. Engelmann, S. et al. The gene for the P-subunit of glycine decarboxylase from the C_4 species *Flaveria trinervia*: analysis of transcriptional control in transgenic *Flaveria bidentis* (C_4) and Arabidopsis (C_3). *Plant Physiology* **146**, 1773–1785 (2008).
6. Gowik, U. et al. *cis*-Regulatory elements for mesophyll-specific gene expression in the C_4 plant *Flaveria trinervia*, the promoter of the C_4 phospho *enol*pyruvate carboxylase gene. *The Plant Cell* **16**, 1077–1090 (2004).
7. Akyildiz, M. et al. Evolution and function of a cis-regulatory module for mesophyll-specific gene expression in the C_4 dicot Flaveria trinervia. *The Plant Cell* **19**, 3391–3402 (2007).
8. Williams, B.P. et al. An untranslated *cis*-element regulates the accumulation of multiple C_4 enzymes in *Gynandropsis gynandra* mesophyll cells. *The Plant Cell* **28**, 454–465 (2016).
9. Brown, N.J. et al. Independent and Parallel Recruitment of Preexisting Mechanisms Underlying C_4 Photosynthesis. *Science* **331**, 1436–1439 (2011).
10. Reyna-Llorens, I. et al. Ancient duons may underpin spatial patterning of gene expression in C_4 leaves. *Proc. Natl Acad. Sci. USA* **115**, 1931–1936 (2018).
11. Matsuoka, M. et al. The promoters of two carboxylases in a C_4 plant (maize) direct cell-specific, light-regulated expression in a C_3 plant (rice). *The Plant Journal* **6**, 311–319 (1994).
12. Kajala, K. et al. Multiple Arabidopsis genes primed for direct recruitment into C_4 photosynthesis. *Plant Journal* **69**, 47–56 (2012).
13. Reyna-Llorens, I. & Hibberd, J.M. Recruitment of pre-existing networks during the evolution of C_4 photosynthesis. *Philosophical Transactions of the Royal Society B: Biological Sciences* **372**, 2–7 (2017).
14. Kinsman, E.A. & Pyke, K.A. Bundle sheath cells and cell-specific plastid development in Arabidopsis leaves. *Development* **125**, 1815–1822 (1998).

15. Shatil-Cohen, A., Attia, Z. & Moshelion, M. Bundle-sheath cell regulation of xylem-mesophyll water transport via aquaporins under drought stress: a target of xylem-borne ABA? *The Plant Journal* **67**, 72–80 (2011).
16. Leegood, R.C. Roles of the bundle sheath cells in leaves of C_3 plants. *Journal of Experimental Botany*, **59**, pp.1663–1673 (2008).
17. Koroleva, O., Farrar, J.F., Tomos, A.D. & Pollock, C.J. Patterns of solute in individual mesophyll, bundle sheath and epidermal cells of barley leaves induced to accumulate carbohydrate. *New Phytol*. **136**, 97–104 (1997).
18. Williams, M., Thomas, B.J., Farrar, J.F. & Pollock, C.J. Visualizing the distribution of elements within barley leaves by energy dispersive X-ray image maps (EDX maps). New Phytol. **125**: 367–372 (2018).
19. Sage, R. Environmental and evolutionary preconditions for the origin and diversification of the C_4 photosynthetic syndrome. *Plant Biology* **3**, 202–213 (2001).
20. Griffiths, H., Weller, G., Toy, L.F.M. & Dennis, R.J. You're so vein: bundle sheath physiology, phylogeny and evolution in C_3 and C_4 plants. *Plant Cell Environ* **36**, 249–261 (2013).
21. Takahashi, H. et al. The roles of three functional sulphate transporters involved in uptake and translocation of sulphate in Arabidopsis thaliana. *Plant Journal* **23**, 171–182 (2000).
22. Kirschner, S. et al. Expression of SULTR2;2, encoding a low-affinity sulphur transporter, in the Arabidopsis bundle sheath and vein cells is mediated by a positive regulator. *Journal of Experimental Botany* **69**, 4897-4906 (2018).
23. Aubry, S., Smith-Unna, R.D., Boursnell, C.M., Kopriva, S. & Hibberd, J.M. Transcript residency on ribosomes reveals a key role for the Arabidopsis thaliana bundle sheath in sulphur and glucosinolate metabolism. *The Plant journal* **78**, 659–673 (2014).
24. Schweizer, F. et al.. Arabidopsis basic helix-loop-helix transcription factors MYC2, MYC3, and MYC4 regulate glucosinolate biosynthesis, insect performance, and feeding behavior. *Plant Cell* **25**, 3117–3132 (2013).
25. Li, B. et al. Promoter-Based Integration in Plant Defense Regulation. *Plant Physiology* **166**, 1803–1820 (2014).
26. Gigolashvili, T., Engqvist, M., Yatusevich, R., Müller, C. & Flügge, U-I. HAG2/MYB76 and HAG3/MYB29 exert a specific and coordinated control on the regulation of aliphatic glucosinolate biosynthesis in Arabidopsis thaliana. *New Phytologist* **177**, 627–642 (2008).
27. Ali, S. & Taylor, W.C. The 3 ' non-coding region of a C_4 photosynthesis gene increases transgene expression when combined with heterologous promoters. *Plant Molecular Biology* **46**, 325–333 (2001).

28. Gallegos, J.E. & Rose, A.B. Intron DNA Sequences Can Be More Important Than the Proximal Promoter in Determining the Site of Transcript Initiation. *The Plant Cell* **29**, 843–853 (2017).
29. Hesselberth, J.R. et al. Global mapping of protein-DNA interactions in vivo by digital genomic footprinting. *Nature methods* **6**, 283–9 (2009).
30. Zhang, W. Zhang, T., Wu, Y. & Jiang, J. Genome-Wide Identification of Regulatory DNA Elements and Protein-Binding Footprints Using Signatures of Open Chromatin in Arabidopsis. *The Plant Cell* **24**, 2719–2731 (2012).
31. Zhang, T., Marand, A.P. & Jiang, J. PlantDHS: a databse for DNase1 hypersensitive sites in plants. *Nucleic Acids Research* **44**, D1148–D1153 (2016).
32. Wysocka-Diller, J.W. Helariutta, Y., Fukaki, H., Malamy, J.E. & Benfey, P.N. Molecular analysis of SCARECROW function reveals a radial patterning mechanism common to root and shoot. *Development* **127**, 595–603 (2000).
33. Grant, C.E., Bailey, T.L. & Noble, W.S. FIMO: scanning for occurrences of a given motif. *Bioinformatics* **27**, 1017–1018 (2011).
34. Fornes, O. et al. JASPAR 2020: update of the open-access database of transcription factor binding profiles. *Nucleic Acids Res*., doi: 10.1093/nar/gkz1001 (2019).
35. Burow, M. et al. The Glucosinolate Biosynthetic Gene AOP2 Mediates Feed-back Regulation of Jasmonic Acid Signaling in Arabidopsis. *Molecular Plant* **8**, 1201–1212 (2015).
36. Sønderby I.E. et al. A systems biology approach identifies a R2R3MYB gene subfamily with distinct and overlapping functions in regulation of aliphatic glucosinolates. *PLoS ONE* **2**, e1322 (2007).
37. Major, I.T. et al. Regulation of growth–defense balance by the JASMONATE ZIM-DOMAIN (JAZ)-MYC transcriptional module. *New Phytologist* **215**, 1533–1547 (2017).
38. Baima, S. et al. The expression of the Athb-8 homeobox gene is restricted to provascular cells in Arabidopsis thaliana. *Development* **121**, 4171–4182 (1995).
39. Levin, J.Z. & Meyerowitz, E.M. UFO - an Arabidopsis Gene Involved In Both Floral Meristem and Floral Organ Development. *Plant Cell* **7**, 529–548 (1995).
40. Fletcher, J.C., Brand, U., Running, M.P., Simon, R. & Meyerowitz, E.M. Signaling of Cell Fate Decisions by CLAVATA3 in Arabidopsis Shoot Meristems. *Science* **19**, 1911–1914 (1999).
41. Otsuga, D., DeGuzman, B., Prigge, M.J., Drews, G.N. & Clark, S.E. REVOLUTA regulates meristem initiation at lateral positions. *The Plant Journal* **25**, 223–236 (2001).
42. Sarkar, A.K. et al. Conserved factors regulate signalling in Arabidopsis thaliana shoot and root stem cell organizers. *Nature* **446**, 811–814 (2007).

770 43. Helariutta, Y. et al. The SHORT-ROOT Gene Controls Radial Patterning of the
771 Arabidopsis Root through Radial Signaling. *Cell* **101**, 555–567 (2000).44.
772 44. Bonke, M., Thitamadee, S., Mähönen, A.P., Hauser, M-T. & Helariutta, Y. APL regulates
773 vascular tissue identity in Arabidopsis. *Nature* **426**, 181–186 (2003).
774 45. Heidstra, R., Welch, D. & Scheres, B. Mosaic analyses using marked activation and
775 deletion clones dissect Arabidopsis SCARECROW action in asymmetric cell division. *Genes*
776 *and Development* **18**, 1964–1969 (2004).
777 46. Mustroph, A. et al. Profiling translatomes of discrete cell populations resolves altered
778 cellular priorities during hypoxia in Arabidopsis. *Proceedings of the National Academy of*
779 *Sciences* **106**, 18843–18848 (2009).
780 47. Ruzicka, D.R. Kandasamy, M.K., McKinney, E.C., Burgos-Rivera, B. & Meagher, R.B.
781 The ancient subclasses of Arabidopsis ACTIN DEPOLYMERIZING FACTOR genes exhibit
782 novel and differential expression. *The Plant Journal* **52**, 460–472 (2007).
783 48. Masucci, J.D. et al. The homeobox gene GLABRA2 is required for position-dependent
784 cell differentiation in the root epidermis of Arabidopsis thaliana. *Development* **122**, 1253–
785 1260 (1996).
786 49. Nakamura, R.L. et al. Expression of an Arabidopsis Potassium Channel Gene in Guard
787 Cells. *Plant Physiology* **109**, 371–374 (1995).
788 50. Imlau, A., Truernit, E. & Sauer, N. Cell-to-Cell and Long-Distance Trafficking of the
789 Green Fluorescent Protein in the Phloem and Symplastic Unloading of the Protein into Sink
790 Tissues. *The Plant Cell* **11**, 309–322 (1999).
791 51. Thoma, S. et al. Tissue-specific expression of a gene encoding a cell wall-localized lipid
792 transfer protein from Arabidopsis. *Plant Physiology* **105**, 35–45 (1994).
793 52. Sparks, E.E. et al. Establishment of expression in the SHORTROOT-SCARECROW
794 transcriptional cascade through opposing activities of both activators and repressors.
795 *Developmental Cell* **39**, 585–596 (2016).
796 53. Neph, S. et al. An expansive human regulatory lexicon encoded in transcription factor
797 footprints. *Nature* **489**, 83–90 (2012).
798 54. Fryer, M.J. et al. Control of Ascorbate Peroxidase 2 expression by hydrogen peroxide
799 and leaf water status during excess light stress reveals a functional organisation of
800 Arabidopsis leaves. *Plant Journal* **33**, 691–705 (2003).
801 55. Bhullar, S. et al. Strategies for Development of Functionally Equivalent Promoters with
802 Minimum Sequence Homology for Transgene Expression in Plants: *cis*-Elements in a Novel
803 DNA Context versus Domain Swapping. *Plant Physiology* **132**, 988-998 (2003).

804 56. Hernandez-Garcia, C.M. & Finer, J.J. Identification and validation of promoters and *cis*-
805 acting regulatory elements. *Plant Science* **217–218**, 109–119 (2014).
806 57. Dey, N., Sarkar, S., Acharaya, S. & Maiti, I.B. Synthetic promoters in planta. *Planta* **242**,
807 1077–1094 (2015).
808 58. Shroff, R., Vergara, F., Muck, A., Svatos, A., and Gershenzon, J. Nonuniform distribution
809 of glucosinolates in *Arabidopsis thaliana* leaves has important consequences for plant
810 defense. *Proc. Natl. Acad. Sci. USA* **105**, 6196–6201(2008).
811 59. Malitsky, S. et al. The Transcript and Metabolite Networks Affected by the Two Clades
812 of Arabidopsis Glucosinolate Biosynthesis Regulators. *Plant Physiology* **148**, 2021-2049
813 (2008).
814 60. Sønderby I.E., Burow, M., Rowe, H.C., Kliebenstein, D.J. & Halkier, B.A. A complex
815 interplay of three R2R3 MYB transcription factors determines the profile of aliphatic
816 glucosinolates in Arabidopsis. *Plant Physiology* **153**, 348–363 (2010).
817 61. Fernández-Calvo, P. et al. The Arabidopsis bHLH transcription factors MYC3 and MYC4
818 are targets of JAZ repressors and act additively with MYC2 in the activation of jasmonate
819 responses. *The Plant Cell* **23**, 701-715 (2011).
820 62. Howe, G.A., Major, I.T. & Koo, A.J. Modularity in jasmonate signaling for multistress
821 resilience. *Annu. Rev. Plant Bio*l. **69**, 387–415 (2018).
822 63. Salehin, M. et al. Auxin-sensitive Aux/IAA proteins mediate drought tolerance in
823 Arabidopsis by regulating glucosinolate levels. *Nature Communications* **10,** 4021 (2019).
824 64. Agarwal, P.K., Gupta, K., Lopato, S. & Agarwal, P. Dehydration responsive element
825 binding transcription factors and their applications for the engineering of stress tolerance.
826 *Journal of Experimental Botany* **68**, 2135–2148 (2017).
827 65. Egawa, C. et al. Differential regulation of transcript accumulation and alternative splicing
828 of a *DREB2* homolog under abiotic stress conditions in common wheat. *Genes & Genetic*
829 *Systems* **81**, 77–91 (2006).
830 66, Qin, F. et al. Regulation and functional analysis of ZmDREB2A in response to drought
831 and heat stresses in Zea mays L. *The Plant Journal* **50**, 54–69 (2007).
832 67. Matsukura, S. et al. Comprehensive analysis of rice DREB2-type genes that encode
833 transcription factors involved in the expression of abiotic stress-responsive genes. *Molecular*
834 *Genetics and Genomics* **283**, 185–196 (2010).
835 68. Vainonen, J.P. et al. RCD1–DREB2A interaction in leaf senescence and stress
836 responses in Arabidopsis *thaliana. Biochemical Journal* **442**, 573-581 (2012).
837 69. Liu, Q. et al. Two Transcription Factors, DREB1 and DREB2, with an EREBP/AP2 DNA
838 Binding Domain Separate Two Cellular Signal Transduction Pathways in Drought- and Low-

839 Temperature-Responsive Gene Expression, Respectively, in Arabidopsis. *The Plant Cell*
840 **10**, 1391-406 (1998).
841 70. Sakuma, Y. et al. Functional Analysis of an Arabidopsis Transcription Factor, DREB2A,
842 Involved in Drought-Responsive Gene Expression. *The Plant Cell* **18**, 1292–1309 (2006).
843 71. Theißen, G., Melzer, R. & Ruümpler, F. MADS-domain transcription factors and the floral
844 quartet model of flower development: Linking plant development and evolution.
845 *Development* **143**, 3259–3271 (2016).
846 72. Sarsby, J., Towers. M.W., Stain, C., Cramer, R. & Koroleva, O.A. Mass spectrometry
847 imaging of glucosinolates in Arabidopsis flowers and siliques. *Phytochemistry* **77**, 110–118
848 (2012).
849 73. Halkier, B.A. & Gershenzon, J. Biology and Biochemistry of Glucosinolates. *Annual*
850 *Review of Plant Biology* **57**, 303–333 (2006).
851 74. Yatusevich, R. et al. Genes of primary sulfate assimilation are part of the glucosinolate
852 biosynthetic network in Arabidopsis thaliana. *Plant Journal* **62**, 1–11 (2010).
853 75. Millard, P.S., Weber, K., Kragelund, B.B. & Burow, M. Specificity of MYB interactions
854 relies on motifs in ordered and disordered contexts. *Nucleic Acids Research* **47,** 9592-9608
855 (2019).
856 76. Adwy, W., Laxa, M. & Peterhansel, C. A simple mechanism for the establishment of C_2-
857 specific gene expression in Brassicaceae. *Plant Journal* **84**, 1231–1238 (2015).
858 77. Mallmann, J. et al. The role of photorespiration during the evolution of C_4 photosynthesis
859 in the genus Flaveria. *eLife* **3**, e02478 (2014).
860 78. Adwy, W., Schlüter, U., Papenbrock, J., Peterhansel, C. & Offermann, S. Loss of the M-
861 box from the glycine decarboxylase P-subunit promoter in C_2 Moricandia species. *Plant*
862 *Gene* **18**, 100176 (2019).
863 79. Nakagawa, T. et al. Development of series of gateway binary vectors, pGWBs, for
864 realizing efficient construction of fusion genes for plant transformation. *J Biosci Bioeng* **104**,
865 34–41 (2007).
866 80. Weber, E., Engler, C., Gruetzner, R., Werner, S. & Marillonnet, S. A Modular Cloning
867 System for Standardized Assembly of Multigene Constructs. *PLOS ONE* **6**, p.e16765
868 (2011).
869 81. Clough, S.J. & Bent, A.F. Floral dip: a simplified method for Agrobacterium-mediated
870 transformation of Arabidopsis thaliana. *Plant Journal* **16**, 735–743 (1998).
871 82. Feike, D. et al. Characterizing standard genetic parts and establishing common
872 principles for engineering legume and cereal roots. *Plant Biotechnology Journal* **17**, 2234–
873 2245 (2019).

83. Patron, N.J. et al. Standards for plant synthetic biology: a common syntax for exchange of DNA parts. *New Phytologist* **208**, 13–19 (2015).
84. Jefferson, R.A., Kavanagh, T.A. & Bevan, M.W. GUS fusions: ß-Glucuronidase as a sensitive and versatile gene fusion marker in higher plants. *EMBO Journal* **6**, 3901–3907 (1987).
85. Deplancke, B. et al. A Gene-Centered C. elegans Protein-DNA Interaction Network. *Cell* **125**, 1193–1205 (2006).
86. Gaudinier, A. et al. Enhanced Y1H assays for Arabidopsis. *Nature methods* **8**, 1053 - 1055 (2011).
87. Pruneda-Paz, J.L. et al. A Genome-Scale Resource for the Functional Characterization of Arabidopsis Transcription Factors. *Cell Reports* **8**, 622–632 (2014).
88. Gaudinier, A., Tang, M., Bågman, A-M. & Brady, S.M. Identification of Protein–DNA Interactions Using Enhanced Yeast One-Hybrid Assays and a Semiautomated Approach. *Methods Mol Biol* **1610**, 187-215 (2017).
89. Du, Z., Zhou, X., Ling, Y., Zhang, Z. & Su, Z. agriGO: a GO analysis toolkit for the agricultural community. *Nucleic Acids Res* **38**, W64–W70 (2010).
90. Bailey, T.L. et al. MEME Suite: tools for motif discovery and searching. *Nucleic Acids Research* **37**, W202–W208 (2009).
91. Castro-Mondragon, J.A., Jaeger, S., Thieffry, D., Thomas-Chollier, M. & van Helden, J. RSAT matrix-clustering: Dynamic exploration and re- dundancy reduction of transcription factor binding motif collections. *Nucleic Acids Res* **45**, e119 (2017).
92. Fornes, O. et al. JASPAR 2020: update of the open-access database of transcription factor binding profiles. *Nucleic Acids Res*., doi: 10.1093/nar/gkz1001 (2019).
93. Quinlan, A.R. & Hall, I.M. BEDTools: a flexible suite of utilities for comparing genomic features. *Bioinformatics* **26**, 841–842 (2010).
94. RStudio Team. RStudio: Integrated Development Environment for R http://www.rstudio.com/ (2015).
95. Robinson, J.T. et al. Integrative genomics viewer. *Nature Biotechnology* **29**, 24 – 26 (2011).

Figure 1: A 468bp region from the *MYB76* promoter necessary for bundle-sheath expression. a) Gene Ontology term enrichment of the 200 most bundle sheath preferential genes in Arabidopsis. Enrichment shown as fold enrichment compared with background. b) Expression of glucosinolate biosynthesis genes in bundle sheath compared with whole leaves. *MYB76* marked in gold, *MYB28* and *MYB29* marked in orange. c) Schematic and representative image of 13 independent T1 lines of the *MYB76* promoter plus 279bp of genomic sequence fused to GUS. d) Schematic and representative image of 12 independent T1 lines of the *MYB76* promoter and full genomic sequence fused to GUS. For C and D staining times are given in the top right corner of each image and scale bars represent 100μm. e) Representative images of 7 independent T1 lines of the *MYB76* promoter driving expression of a histone GFP fusion. Images of the vascular bundle (left) and mesophyll (right). Black arrowheads indicate nuclei expressing GFP. f) Schematics and representative GUS images of 13, 11, and 11 independent T1 lines respectively of each *MYB76* deletion. Staining times are given in the top right corner of each image. Scale bars represent 100μm.

Figure 2: A DNaseI Hypersensitive Site in the *MYB76* promoter is necessary and sufficient for expression in the bundle-sheath. a) The *MYB76* promoter contains a DNaseI Hypersensitive Site (DHS) located between nucleotides -909 to -654. The y-axis shows the DHS score[31] from flower buds (top) and leaves (bottom). Data are from Zhang et al., (2012)[30] visualised with the IGV browser[95]. b) Schematics and representative GUS staining images of 6, 13, and 13 independent T1 lines respectively of the *MYB76* promoter with the DHS deleted, the DHS fused to the minimal *CaMV35S* promoter and two copies of the DHS fused to the minimal *CaMV35S* promoter. Staining times are given in the top right corner of each image. Scale bars represent 100μm. c) Position Weight Matrices (PWMs) of two motifs (1 and 2) found in the *MYB76* DHS as well as other promoters driving bundle sheath expression in Arabidopsis and a 27bp region of the *MYB76* DHS containing motif 2 (TGCACCG) and highlighted in colours matching the PWM. A predicted MYC transcription factor binding site is underlined. d) Schematics and representative images of 13, 13, and 8 independent T1 lines respectively of *MYB76* promoter and gDNA (top), *MYB76* promoter and genomic DNA with the TGCACCG motif deleted (middle), and oligomerisation of the 27bp region containing TGCACCG (bottom) fused to GUS. Staining times are given in the top right corner of each image. Scale bars represent 200μm.

Figure 3: MYC, MYB and DREB transcription factors control *MYB76* expression from the DHS. a) Transcription factor binding motifs within the *MYB76* DHS. Position in the DHS (bp) is on the x-axis, and predicted binding affinity (p-values calculated from log-likelihood score by the FIMO tool[33]) on the y-axis. Motifs are coloured by motif cluster (Supplementary Table 1). The gold region represents the 27bp region necessary for expression and the grey region indicates sequence unable to generate bundle sheath expression (Figure 1f). b) Summary of candidate transcription factors binding to the *MYB76* DHS. Information provided includes gene identifier, gene name, family, expression in bundle sheath compared with whole leaves[23], whether they interacted with the DHS in Yeast One-Hybrid, whether they were previously identified as binding the entire *MYB76* promoter[25], and if they have previously been associated with controlling *MYB76* expression[24,26]. c) *Trans*-activation assays of candidate transcription factors and the *MYB76* DHS. Values shown represent the log of LUCIFERASE (LUC) signal driven by *MYB76DHS::LUC* normalised to a constitutively expressed GUS infiltration control. Box-plots show inter-quartile range as upper and lower confines of the box, median as a solid black line, mean as a white diamond and whiskers as maximum and minimum values excluding outliers. All individual data points are plotted. a, b, c and d represent statistically significant differences ($p<0.05$) as determined by two-sided, pairwise T-tests. p-value versus DHS control for DREB2A is 0.0136, MYC2 is 1.1e-05, MYC3 is 3.2e-09and MYC4 is 2.2e-05. n = independent biological samples with n=3 for DREB2A, DREB26 and MYC4, n=4 for MYC2, DF1 and MYB73, n=6 for MYC3 and n=7 for DHS. d) qRT-PCR of *MYB76* in WT, *dreb2a* and *myc2/3/4*. Expression shown relative to *APA1,* n=6 independent biological samples for all genotypes. Box-plots show inter-quartile range as upper and lower confines of the box, median as a solid black line, mean as a white diamond and whiskers as maximum and minimum values excluding outliers. All individual data points are plotted. All individual data points are plotted. a, b and c represent statistically significantly differences ($p<0.05$) determined by two-sided, pairwise T-tests. p-value versus WT for *dreb2a* is 0.013 and for *myc2/3/4* is 0.0011. e) *MYB76* expression from a publically available *myb28/29* transcriptome[35]. Expression in WT (left) shown as log counts per million. Expression in *myb28/29* (right) shown as log fold change relative to wild type. f) A simplified model (after [24,25,35]) showing activation of aliphatic glucosinolate biosynthesis genes by MYC and MYB transcription factors. g) Schematic showing the relationship between the model presented in (f) and *MYB76* expression in the bundle sheath. Promoters are represented by grey boxes, the DHS by a white box, and the CaMV35S minimal promoter by a black box. GUS staining images for the constructs referred to in the schematic are found (from top to bottom) in Figures 1c, 1f, 2b and 2d.

Figure 4: The MYC-MYB module controls bundle sheath expression of multiple genes. a, b, c) Change in expression in *myc2/3/4* compared with wild type[37] plotted against that of *myb28/29* compared with wild type[35]. Down-regulated genes (log2 < -0.75) in *myc2/3/4* only (a), *myb28/29* only (b) and in both *myc2/3/4* and *myb28/29* (c) are marked in red. d, e, f) Density plots for down-regulated genes highlighted in a, b and c indicating their expression in bundle sheath cells compared with whole leaves[23]. g, h, i) Enrichment analysis of motif clusters found in promoters of down-regulated genes highlighted in a (207 genes), b (729 genes) and c (76 genes). Clusters containing possible MYC binding sites (G-boxes) (Clusters 6 and 8) and MYB binding sites (Clusters 10 and 18) are highlighted in red. Note that Clusters 6, 8, 10 and 18 are strongly enriched in genes down-regulated in both *myc2/3/4* and *myb28/29*. Box-plots show inter-quartile range as upper and lower confines of the box, median as a solid black line and whiskers as maximum and minimum values excluding outliers. Number of motifs per cluster can be found in Supplementary Table 1. j) Violin plots depicting minimum distance (log bp) between cluster 8 and 18 motifs in promoters of genes highlighted in a, b, c and in four random sets of genes from Arabidopsis, ordered by median from smallest to largest. The median is shown as a horizontal black line, the mean as a white diamond. a and b indicate statistically significant differences ($p < 0.05$) determined by two-sided, pairwise Wilcoxon rank-sum tests. p-values for *myc2/3/4* and *myb28/29* = 0.0026 versus random set a, 0.0111 versus random set b, 0.0128 versus random set c, 0.0147 versus random set d, 0.0018 versus *myb28/29,* and 0.0026 versus *myc2/3/4*. n = individual genes tested. n=53 for genes down-regulated in *myc2/3/4* and *myb28/29*, n=506 for genes down=regulate only in *myb28/29*, n=101 in genes down-regulated only in *myc2/3/4* and n=66 for each of the random sets of Arabidopsis genes.

Supplementary Table 1

Clustering of the Arabidopsis motifs from the JASPAR database[92].

Supplementary Table 2

Genes down-regulated only in the *myc2/3/4* mutant[37], the *myb28/29* mutant[35] or in both *myc2/3/4* and *myb28/29* mutants.

Supplementary Table 3

Transcript abundance in bundle sheath and CaMV35S lines[23] for genes down-regulated only in the *myc2/3/4* mutant[37], the *myb28/29* mutant[35] or in both *myc2/3/4* and *myb28/29* mutants.

Supplementary Table 4

Positive interactions determined by Yeast One-Hybrid using the *MYB76* DHS as bait.

Supplementary Table 5

List of primers used in this study.

Supplementary Table 6

Tables of p values associated with Figures 3c, 3d, and 4j.

a

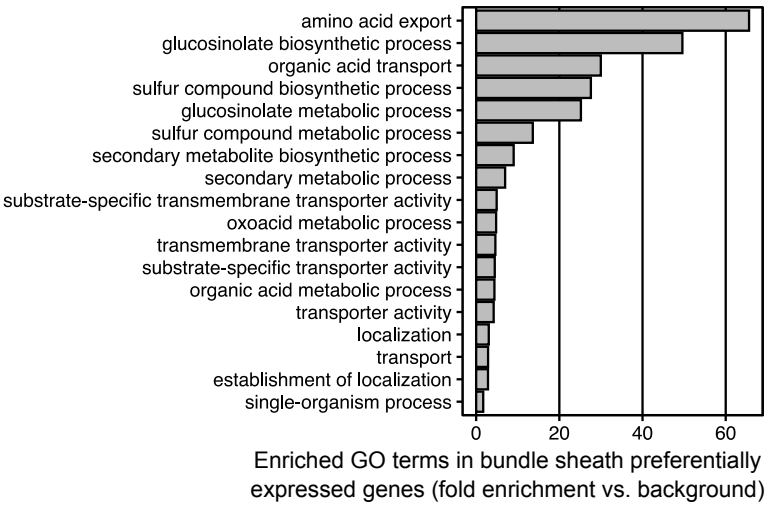
amino acid export
glucosinolate biosynthetic process
organic acid transport
sulfur compound biosynthetic process
glucosinolate metabolic process
sulfur compound metabolic process
secondary metabolite biosynthetic process
secondary metabolic process
substrate-specific transmembrane transporter activity
oxoacid metabolic process
transmembrane transporter activity
substrate-specific transporter activity
organic acid metabolic process
transporter activity
localization
transport
establishment of localization
single-organism process
0
20
40
60
Enriched GO terms in bundle sheath preferentially expressed genes (fold enrichment vs. background)

b

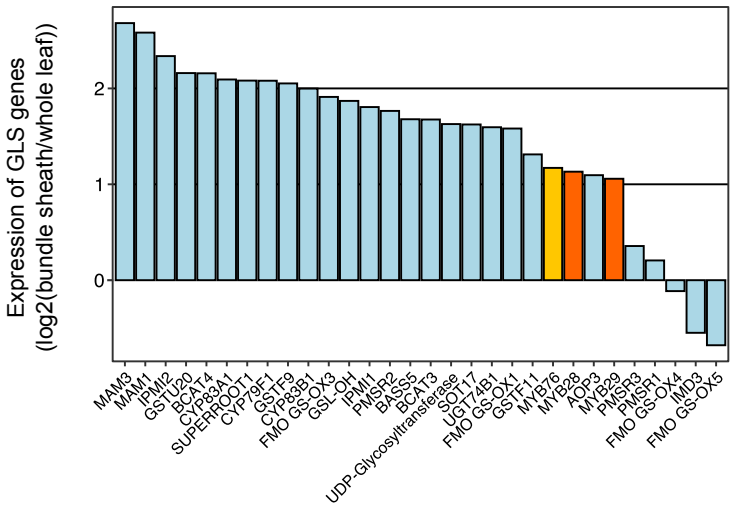
Expression of GLS genes (log2(bundle sheath/whole leaf))
2
1
0
MAM3
MAM1
IPMI2
GSTU20
BCAT4
CYP83A1
SUPERROOT1
CYP79F1
GSTF9
CYP83B1
FMO GS-OX3
GSL-OH
IPMI1
PMSR2
BASS5
BCAT3
UDP-Glycosyltransferase
SOT17
UGT74B1
FMO GS-OX1
GSTF11
MYB76
MYB28
AOP3
MYB29
PMSR3
PMSR1
FMO GS-OX4
IMD3
FMO GS-OX5

c


-1725
ATG
+279

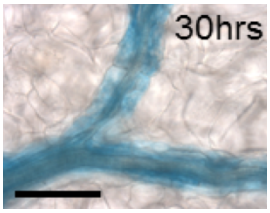
30hrs

d

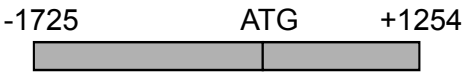
-1725
ATG
+1254

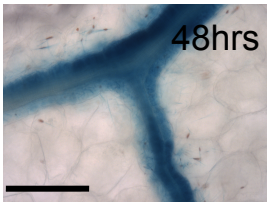
48hrs

e

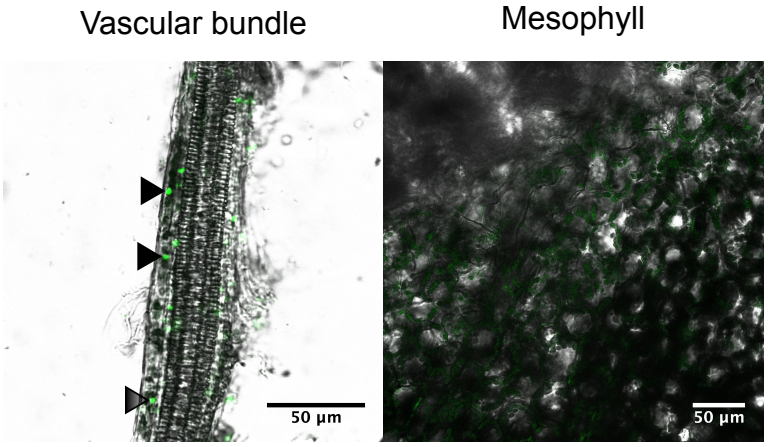
Vascular bundle
Mesophyll
50 µm
50 µm

f


-1264
ATG
+279

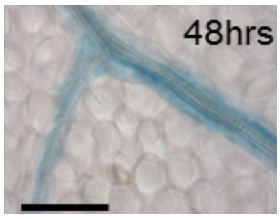
48hrs


-796
ATG
+279

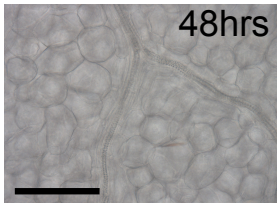
48hrs

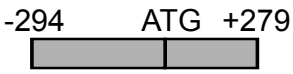
-294
ATG
+279

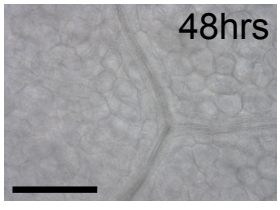
48hrs

a

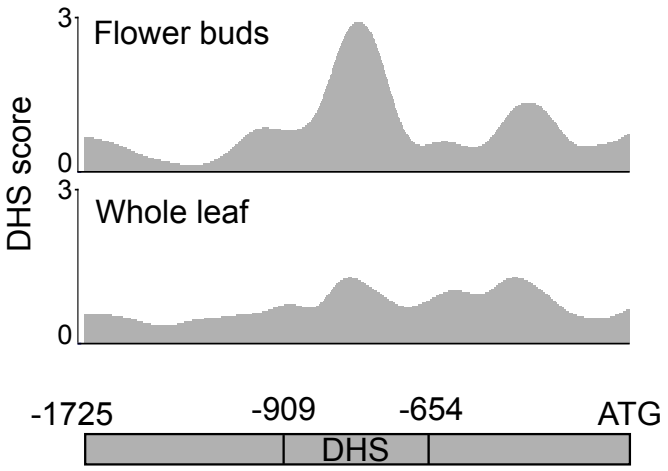

b

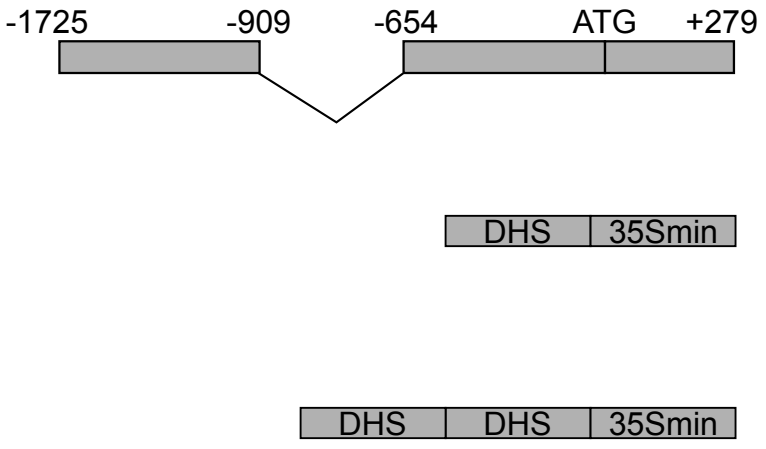

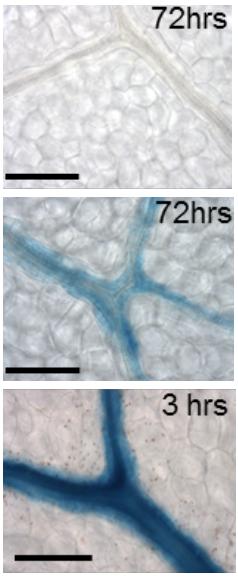

c

Motif 1

Motif 2

27bp region CCGAAAAACGTGCACCGTCCAAGATTC

d

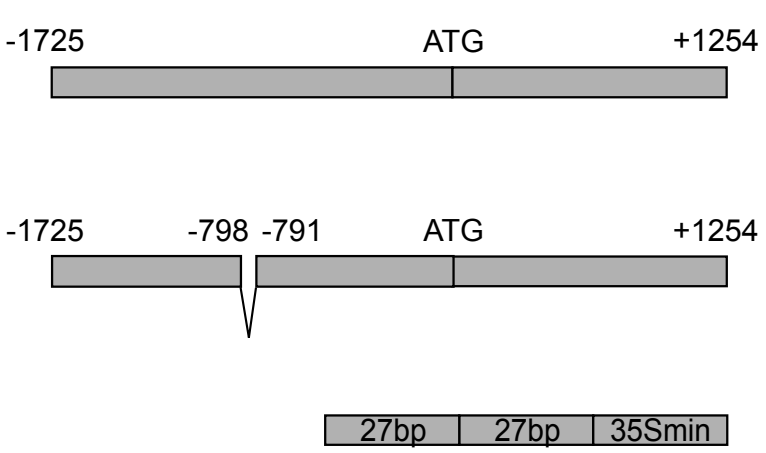

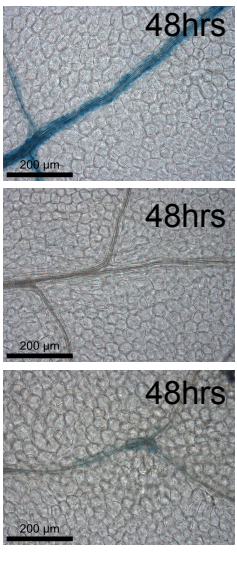

a

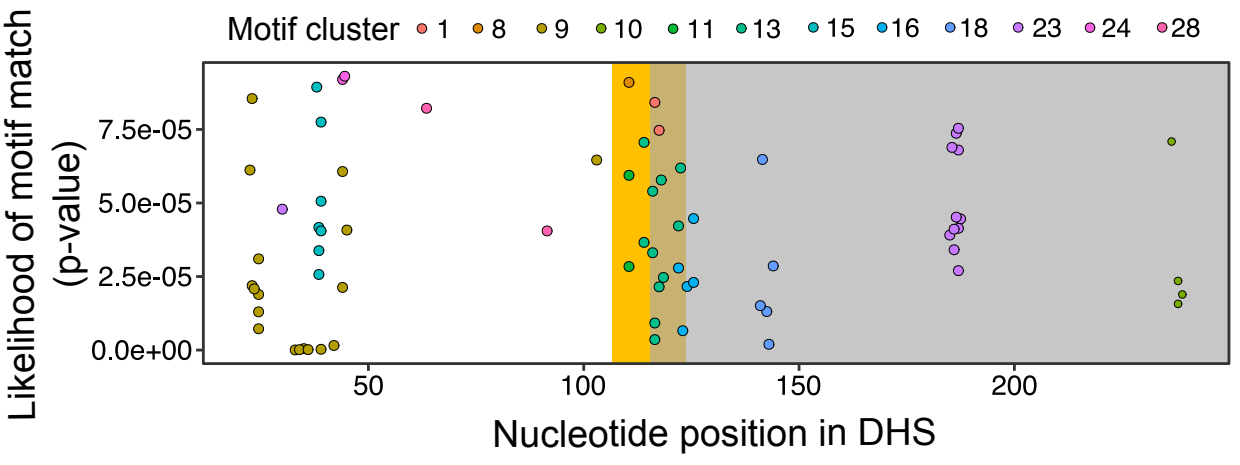

b

Gene id	Name	Family	log2(BS/35S)	Y1H this study	Y1H (Li et al., 2014)	Previously associated with *MYB76*
AT1G32640	MYC2	bHLH		N	N	Y
AT5G46760	MYC3	bHLH		N	N	Y
AT4G17880	MYC4	bHLH		N	N	Y
AT5G61420	MYB28	MYB		N	N	Y
AT5G07690	MYB29	MYB		N	N	Y
AT5G07700	MYB76	MYB		N	N	Y
AT1G21910	DREB26	AP2-EREBP		Y	Y	N
AT1G54060	ASIL1	Trihelix		Y	Y	N
AT1G76880	DF1	Trihelix		Y	Y	N
AT2G22840	GRF1	GRF		Y	Y	N
AT4G37260	MYB73	MYB		Y	Y	N
AT5G52020	RAP2.10	AP2-EREBP		Y	Y	N
AT5G63790	NAC102	NAC		Y	Y	N
AT1G43700	VIP1	bZIP		Y	N	N
AT2G31230	ERF15	AP2-EREBP		Y	N	N
AT2G46270	GBF3	bZIP		Y	N	N
AT3G61830	ARF18	ARF		Y	N	N
AT5G05410	DREB2A	AP2-EREBP		Y	N	N
AT5G57390	AIL5	AP2-EREBP		Y	N	N

c

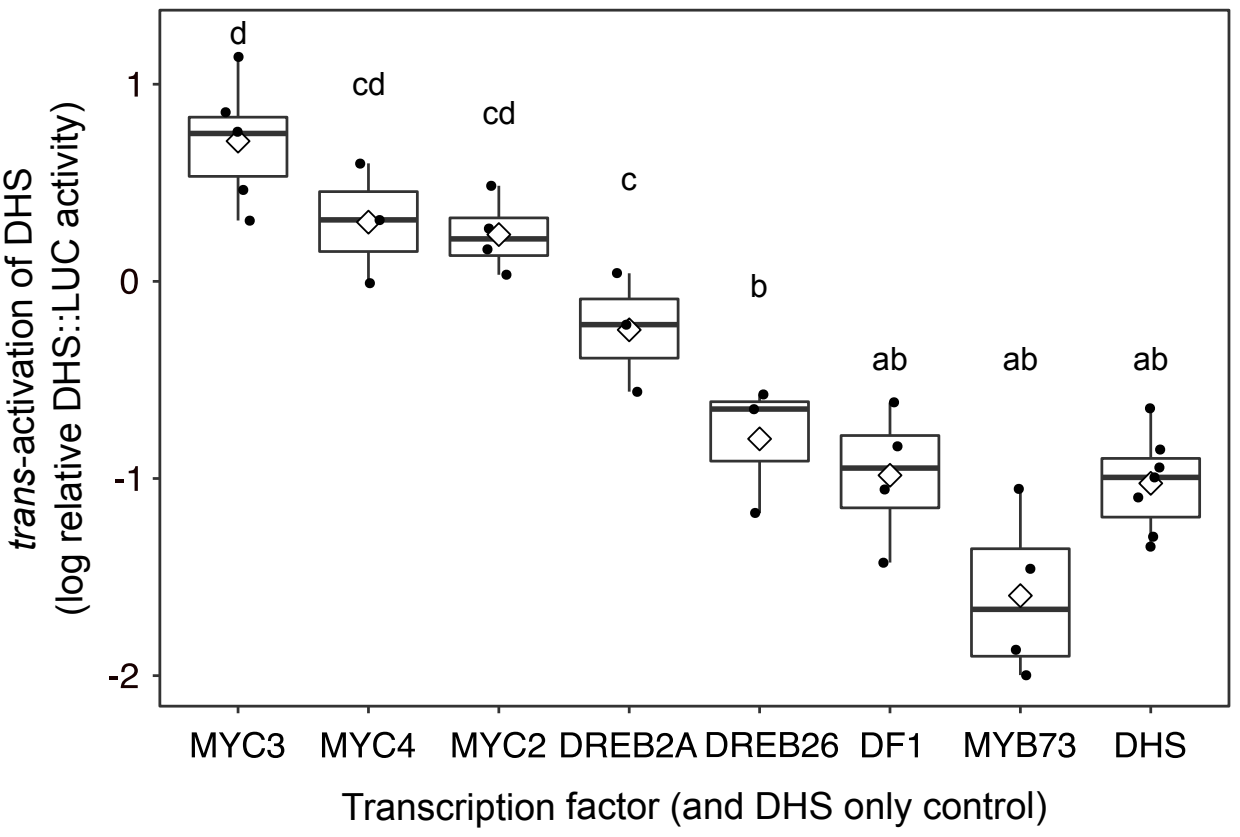

d

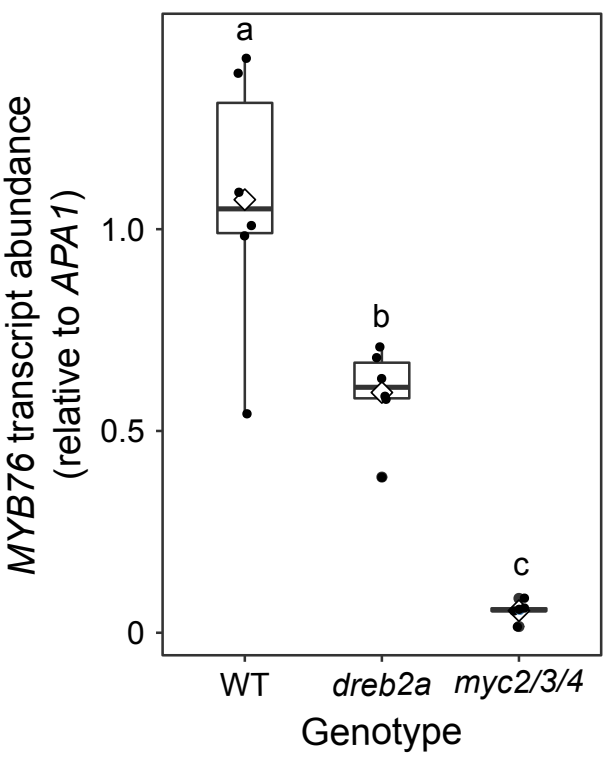

e

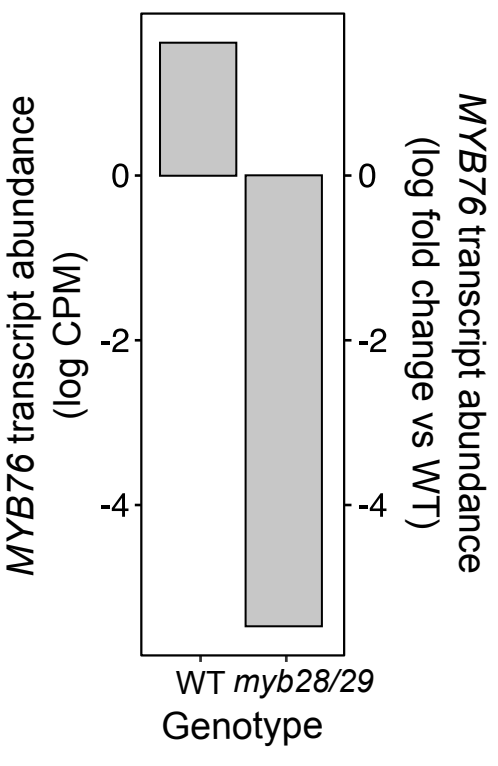

f

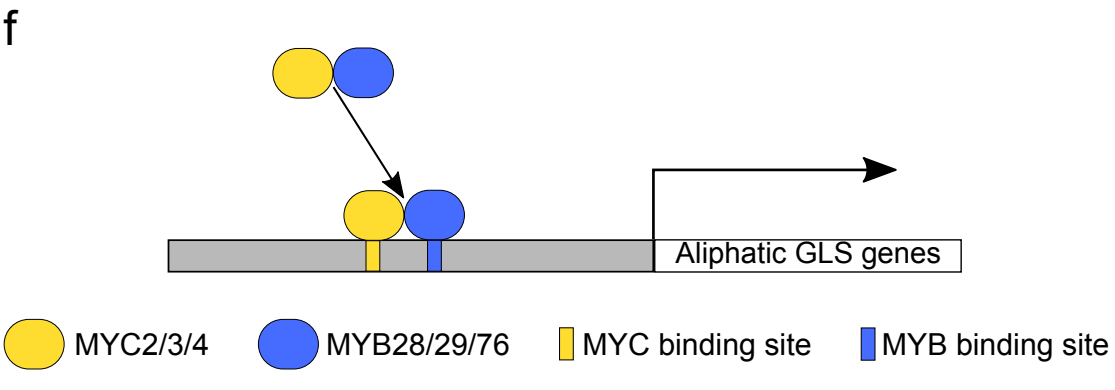

g

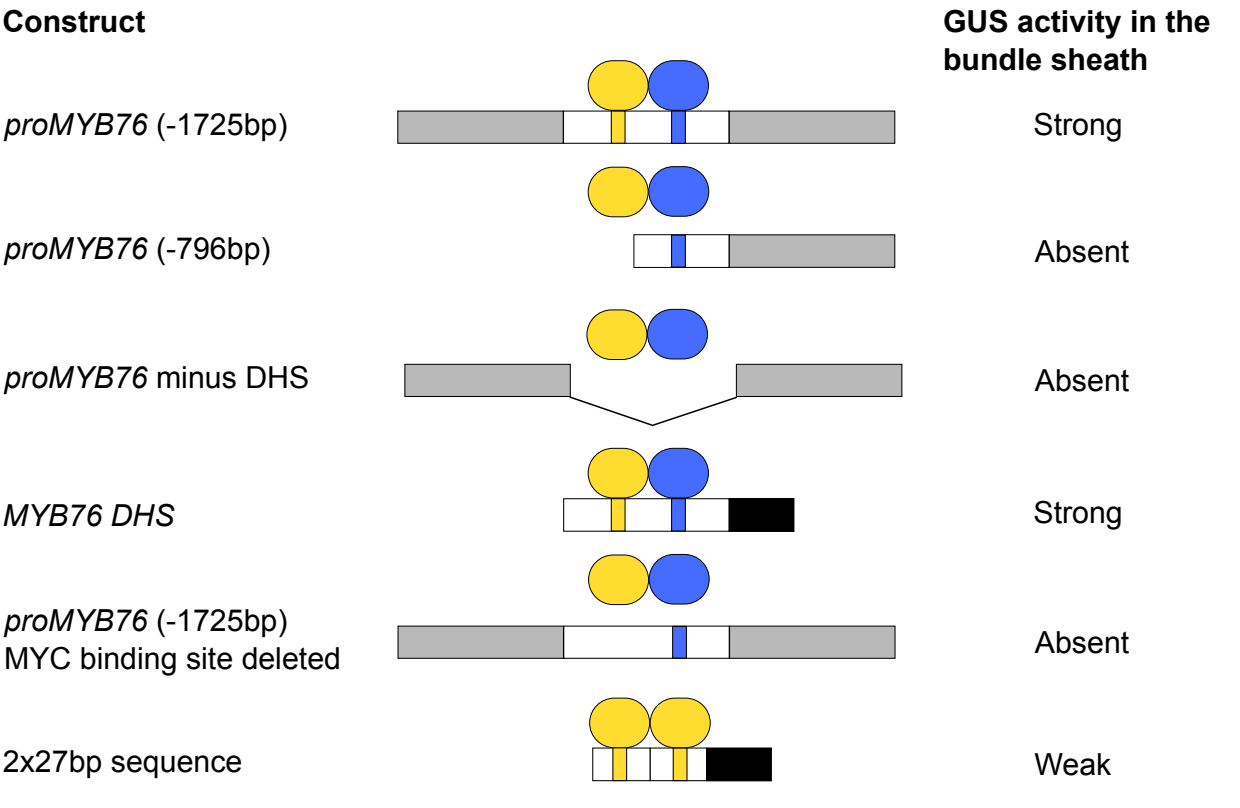

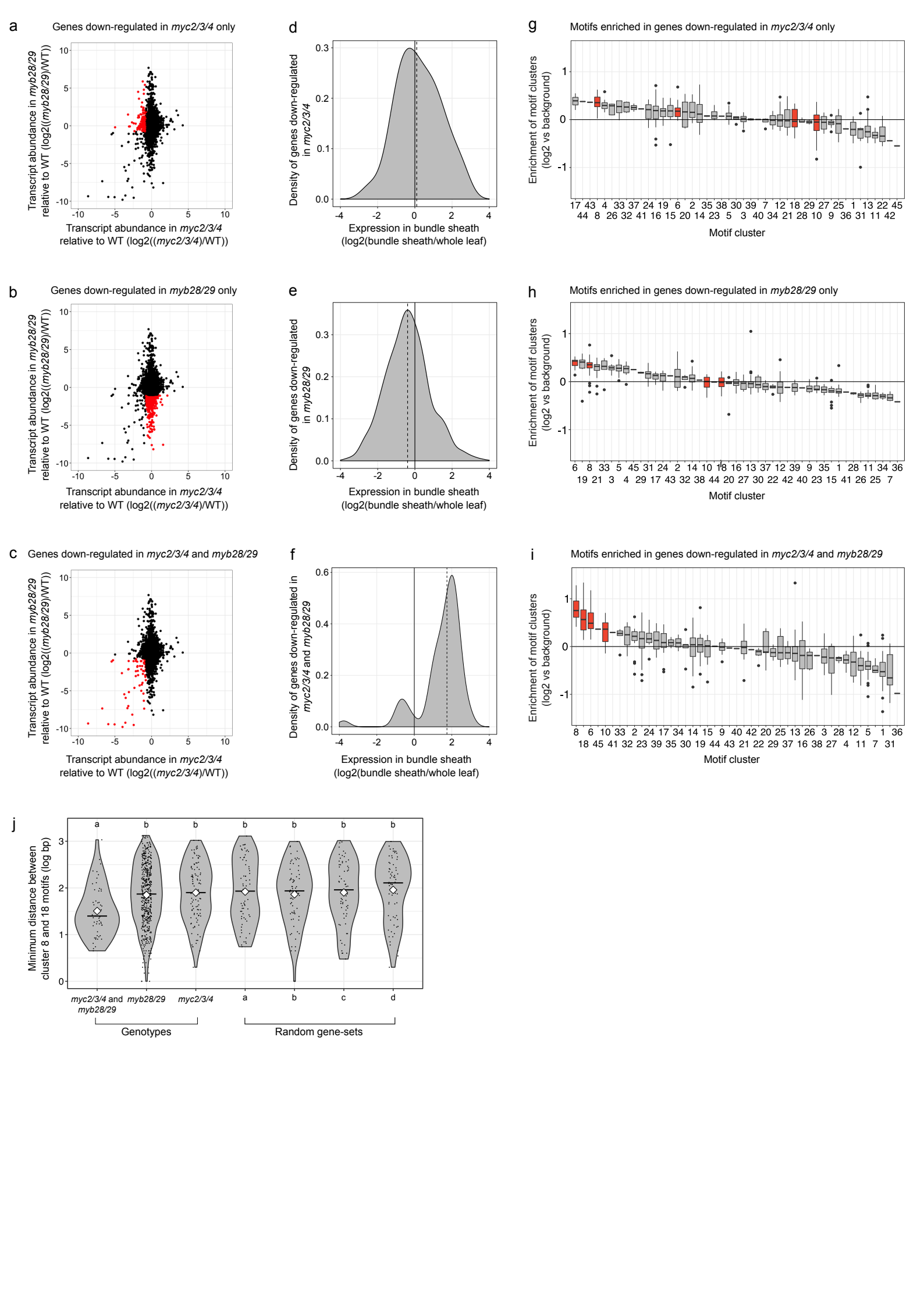
a
Genes down-regulated in myc2/3/4 only
Transcript abundance in myb28/29 relative to WT (log2((myb28/29)/WT))
Transcript abundance in myc2/3/4 relative to WT (log2((myc2/3/4)/WT))
b
Genes down-regulated in myb28/29 only
c
Genes down-regulated in myc2/3/4 and myb28/29
d
Density of genes down-regulated in myc2/3/4
Expression in bundle sheath (log2(bundle sheath/whole leaf)
e
Density of genes down-regulated in myb28/29
f
Density of genes down-regulated in myc2/3/4 and myb28/29
g
Motifs enriched in genes down-regulated in myc2/3/4 only
Enrichment of motif clusters (log2 vs background)
17 43 4 33 37 24 19 6 2 35 38 30 39 7 12 18 29 27 25 1 13 22 45
44 8 26 32 41 16 15 20 14 23 5 3 40 34 21 28 10 9 36 31 11 42
Motif cluster
h
Motifs enriched in genes down-regulated in myb28/29 only
6 8 33 5 45 31 24 2 14 10 18 16 13 37 12 39 9 35 1 28 11 34 36
19 21 3 4 29 17 43 32 38 44 20 27 30 22 42 40 23 15 41 26 25 7
i
Motifs enriched in genes down-regulated in myc2/3/4 and myb28/29
8 6 10 33 2 24 17 34 14 15 9 40 42 20 25 13 26 3 28 12 5 1 36
18 45 41 32 23 39 35 30 19 44 43 21 22 29 37 16 38 27 4 11 7 31
j
Minimum distance between cluster 8 and 18 motifs (log bp)
a b b b b b b
myc2/3/4 and myb28/29
myb28/29
myc2/3/4
a
b
c
d
Genotypes
Random gene-sets

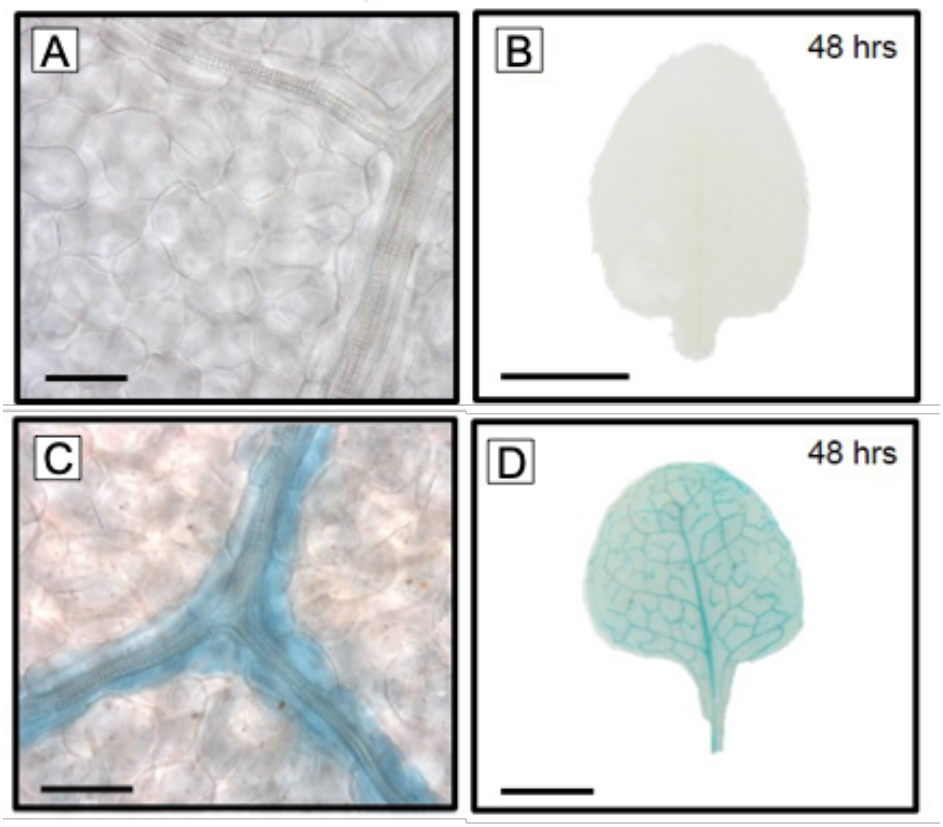

Supplementary Figure 1: Representative images from 10, and 10 independent T1 lines respectively of *proMYB*28 and *proMYB29* GUS. Staining performed for 48hrs and scale bars represent 0.5 cm (a and c) and 50 µm (b and d).

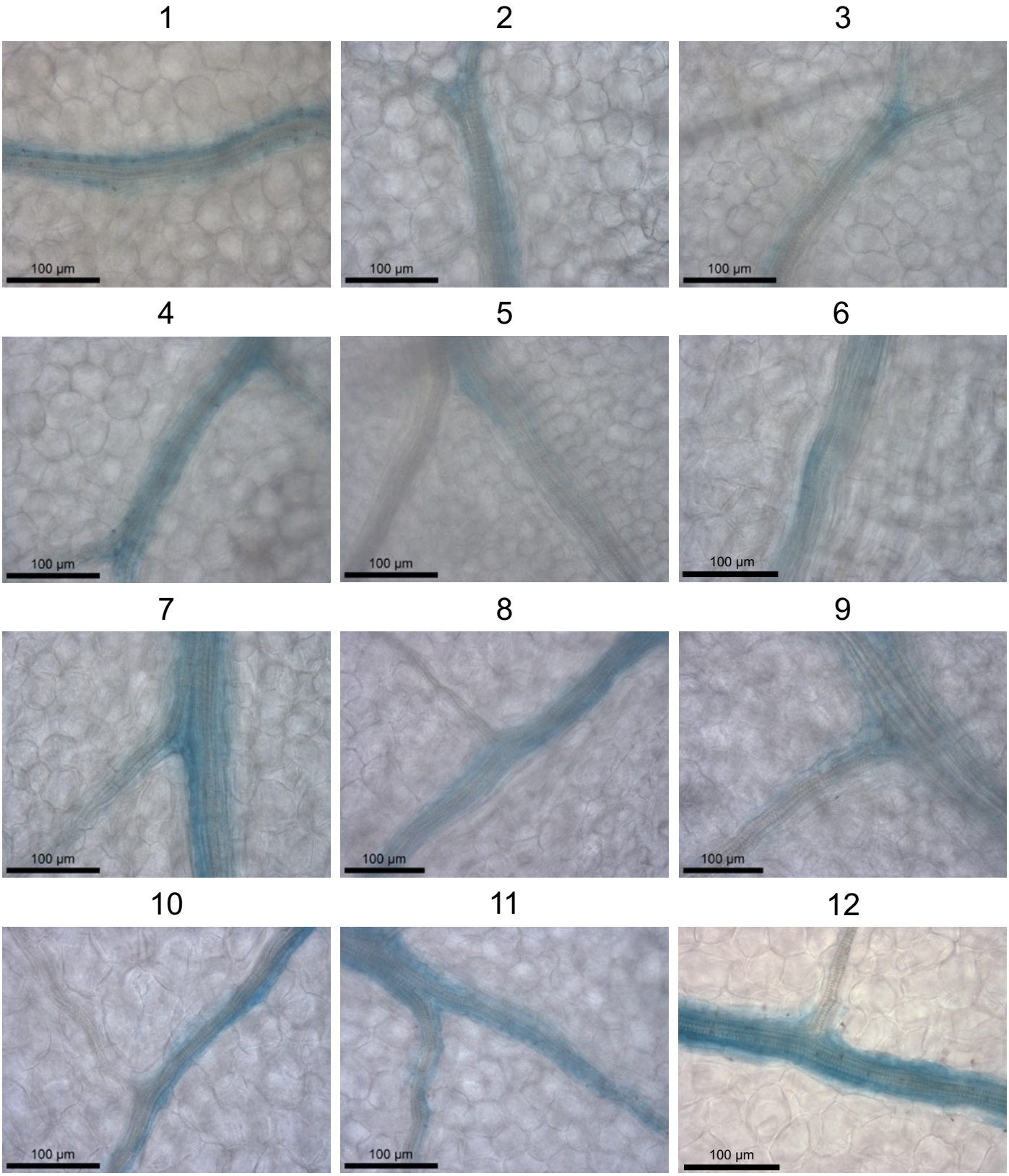

Supplementary Figure 2: Nucleotides -1725 to +279 relative to the predicted translational start site of *MYB76* generate preferential expression in the bundle sheath. Images from 12 independent transgenic lines. Leaves were stained for 30hrs. Scale bars represent 100 µm.

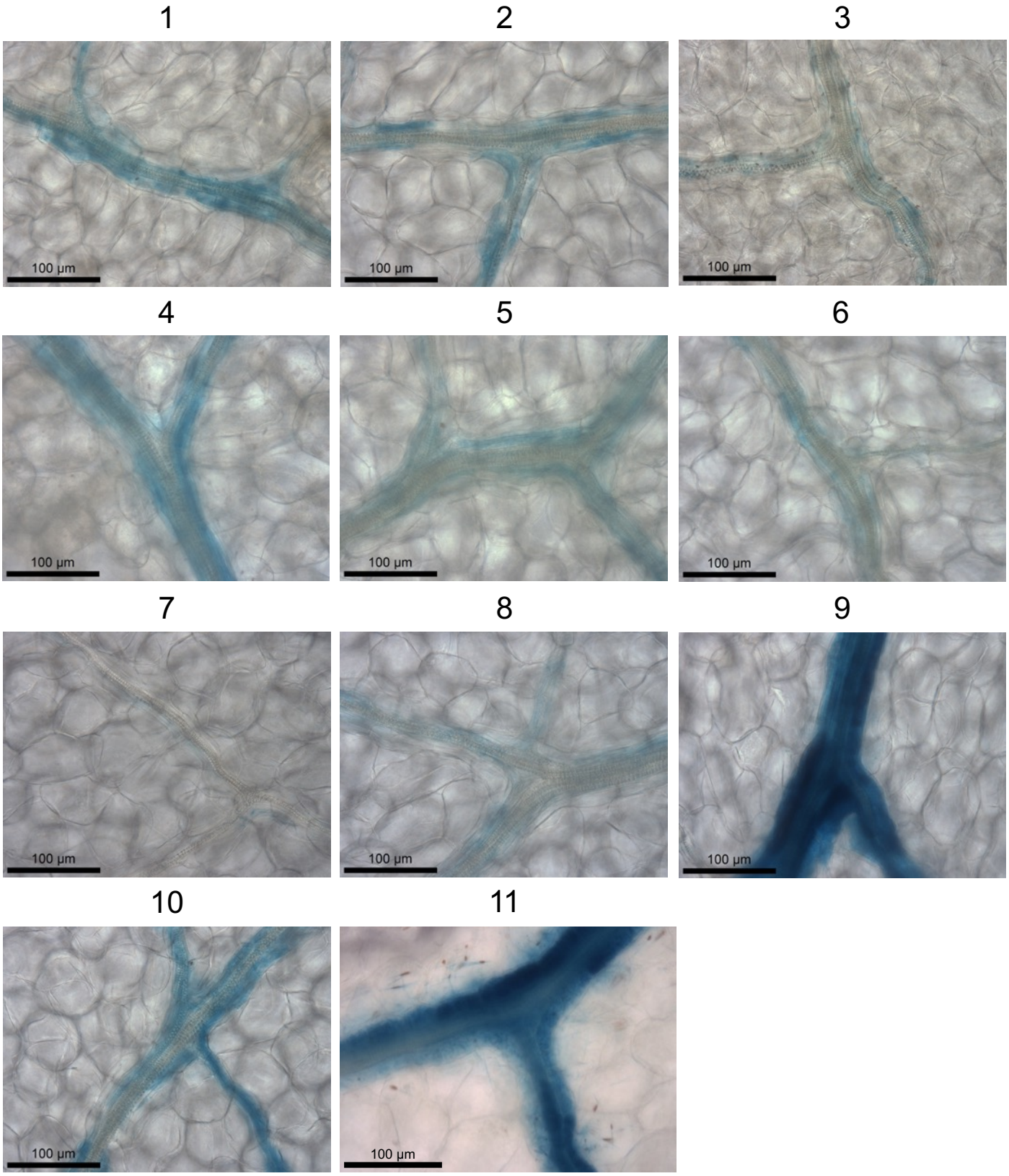

Supplementary Figure 3: The genomic *MYB76* sequence fused to GUS generates preferential expression in the bundle sheath. Images from 11 independent transgenic lines Leaves were stained for 72hrs except line 11 which was stained for 48hrs. Scale bars represent 100 µm.

a

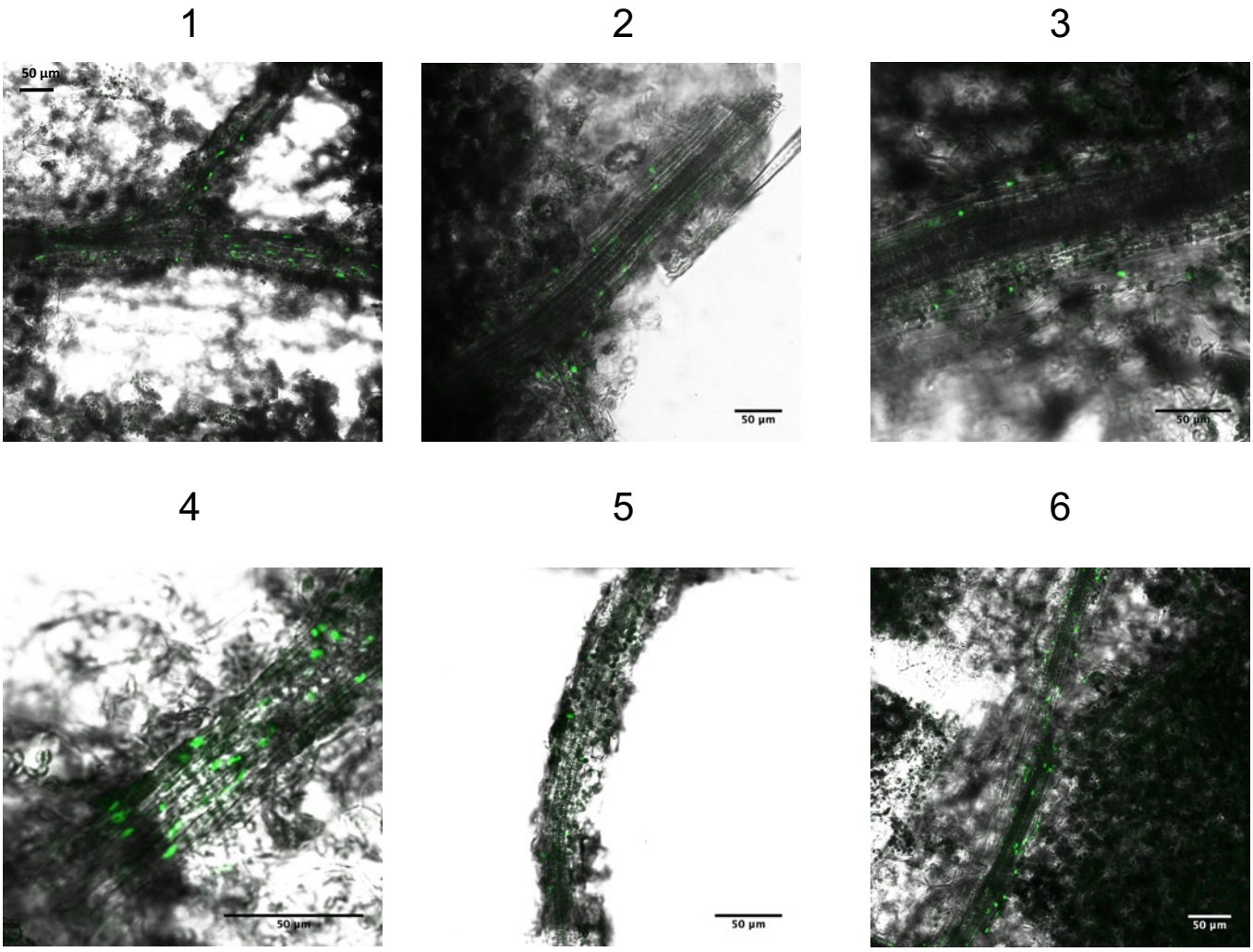

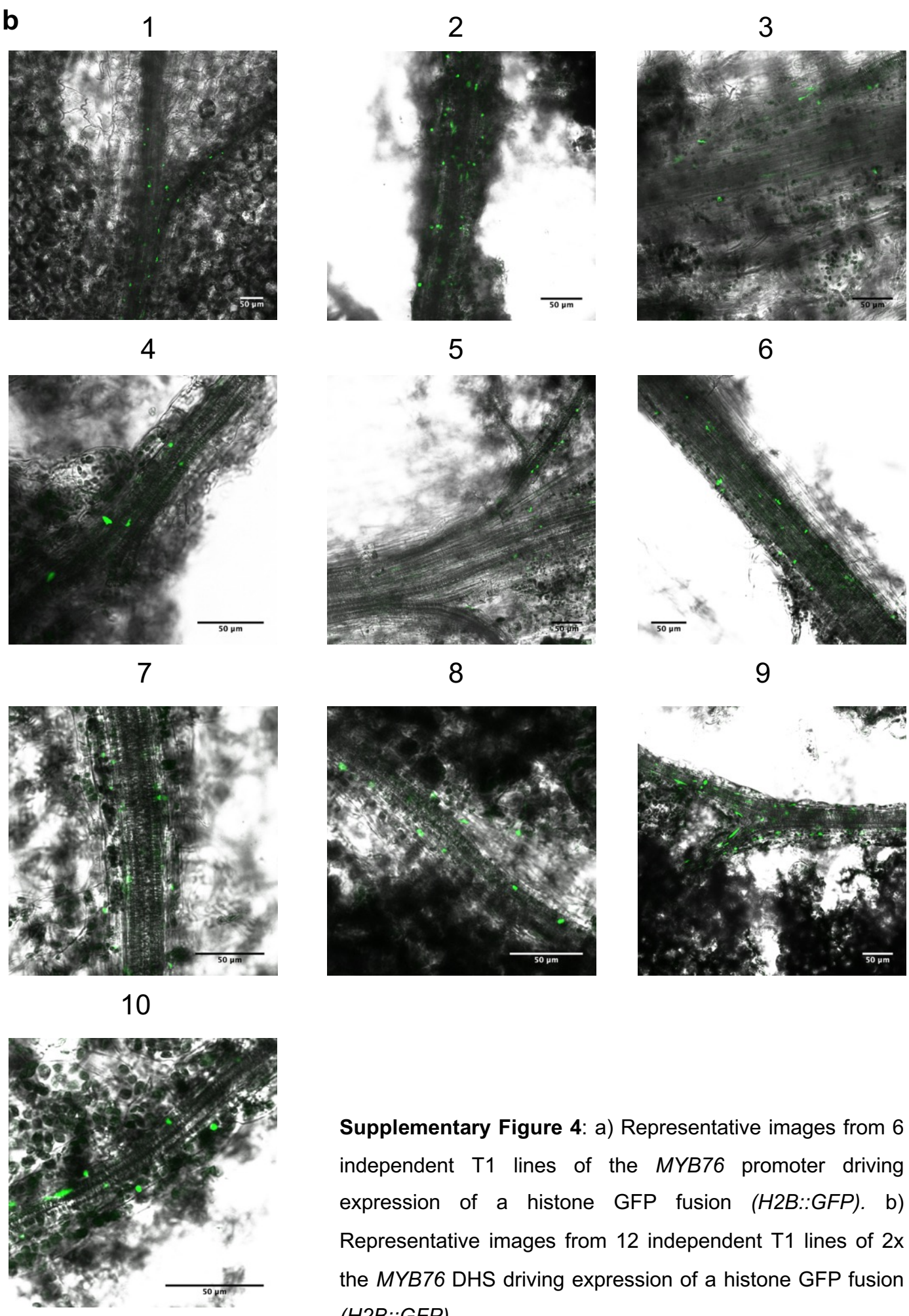

Supplementary Figure 4: a) Representative images from 6 independent T1 lines of the *MYB76* promoter driving expression of a histone GFP fusion *(H2B::GFP).* b) Representative images from 12 independent T1 lines of 2x the *MYB76* DHS driving expression of a histone GFP fusion *(H2B::GFP).*

a

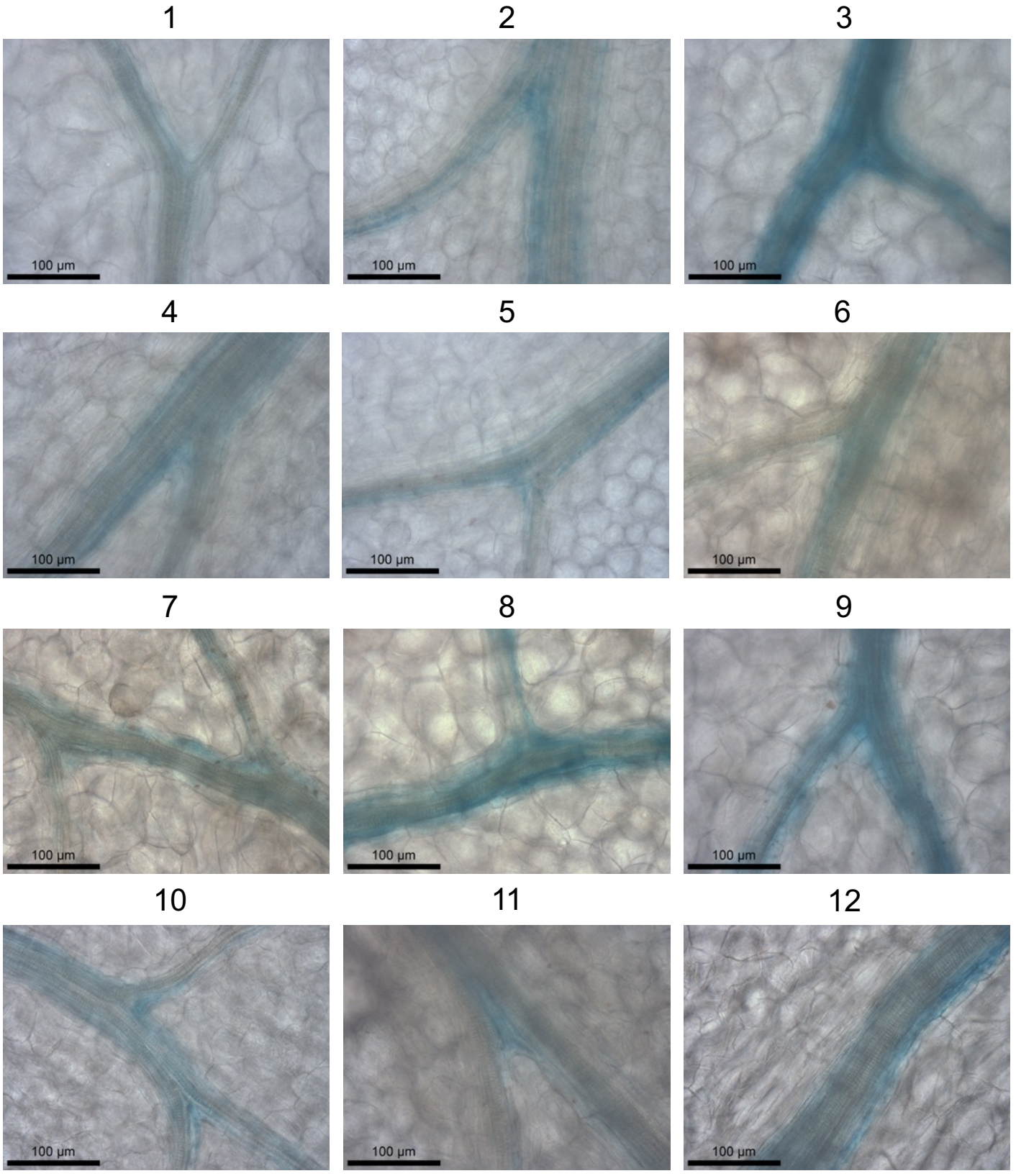

b

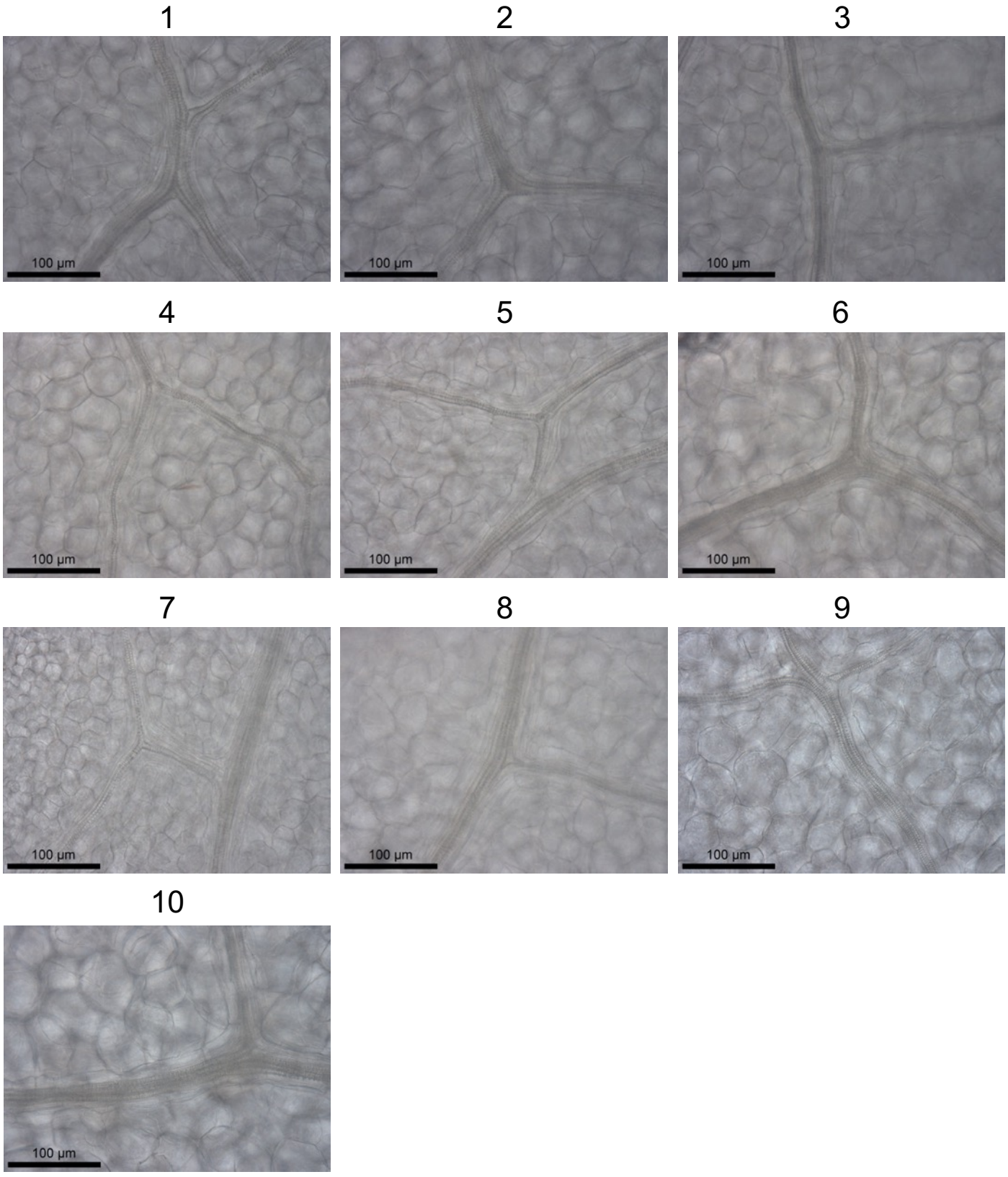

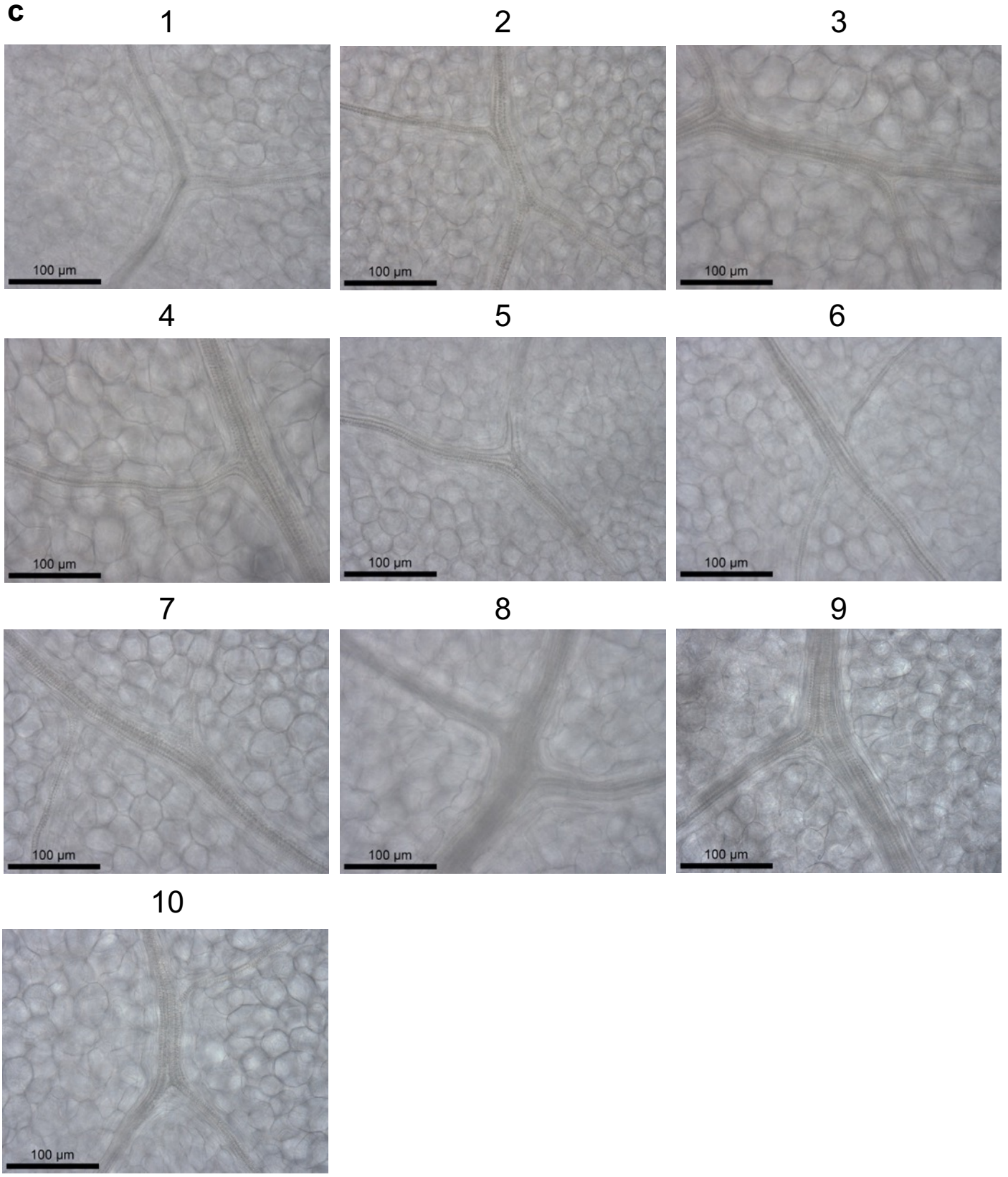

Supplementary Figure 5: a) Nucleotides -1264 to +279 relative to the predicted translational start site of MYB76 generate preferential expression in the bundle sheath. Images from 12 independent transgenic lines. b) 796bp of the promoter combined with the first exon and intron of *MYB76* does not generate BS preferential expression. Images from 10 independent transgenic lines. c) 294bp of the promoter combined with the first exon and intron of *MYB76* does not generate BS preferential expression. Images from 10 independent transgenic lines. Leaves were stained for 48hrs. Scale bars represent 100 µm.

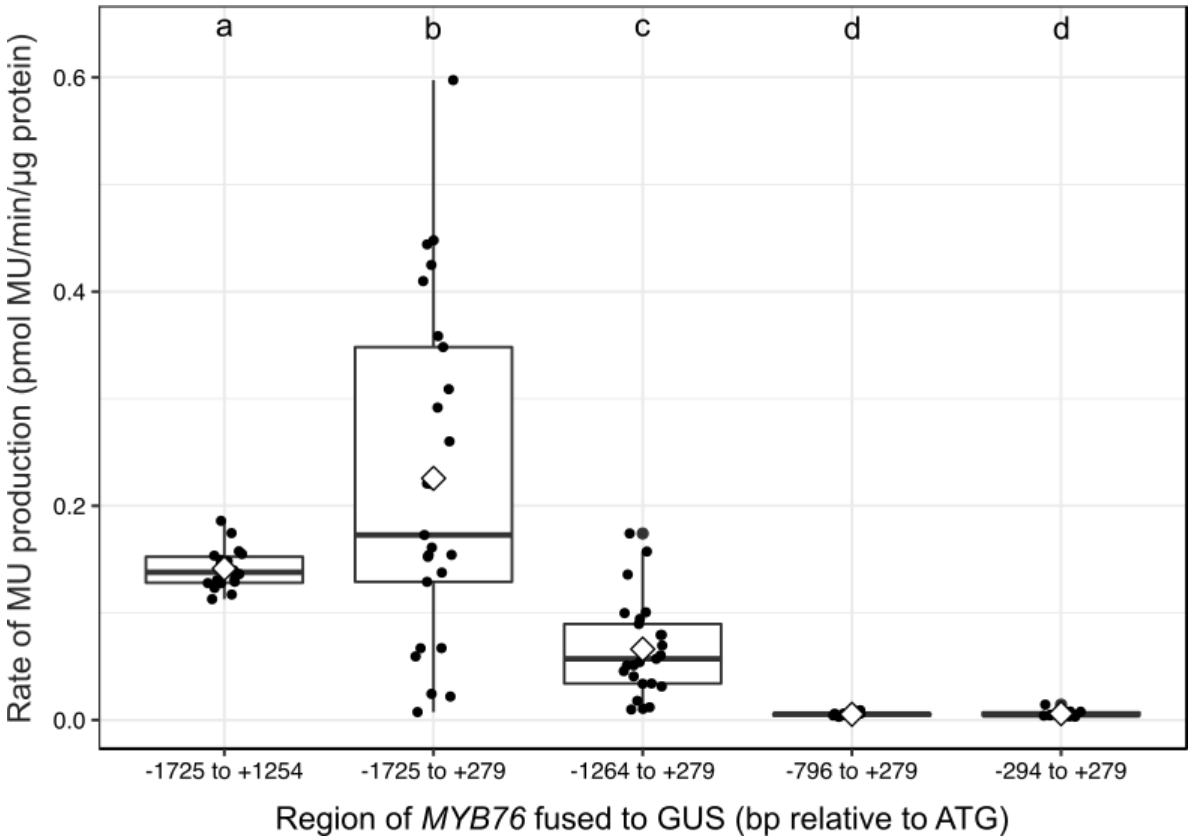

p values from pairwise, two sided, T tests				
	-1264 to +279	**-1725 to +1254**	**-1725 to +279**	**-294 to +279**
-1725 to +1254	0.000000042	-	-	-
-1725 to +279	0.00013	0.02866	-	-
-294 to +279	0.0000022	4.1E-16	0.0000022	-
-796 to +279	0.0000022	1.7E-15	0.0000022	0.60967

Supplementary Figure 6: Quantification of MUG activity via the flourometric MUG assay for multiple independent T1 transformants of *MYB76* GUS reporters from Figure 1. The MUG assays show quantitative repressors and enhancers are located in the gene and in the promoter respectively. n=18 for -1725 to +1254, 25 for -1725 to +297, 25 for -1264 to +279, 10 for -796 to +279 and 10 for -294 to +279. a, b, c and d represent significantly different groups ($p<0.05$) determined by pairwise two-sided, T-tests. Box-plots show inter-quartile range as upper and lower confines of the box, median as a solid black line, mean as a white diamond and whiskers as maximum and minimum values excluding outliers. All individual data points are plotted. The table below the plot shows p values of all comparisons.

a

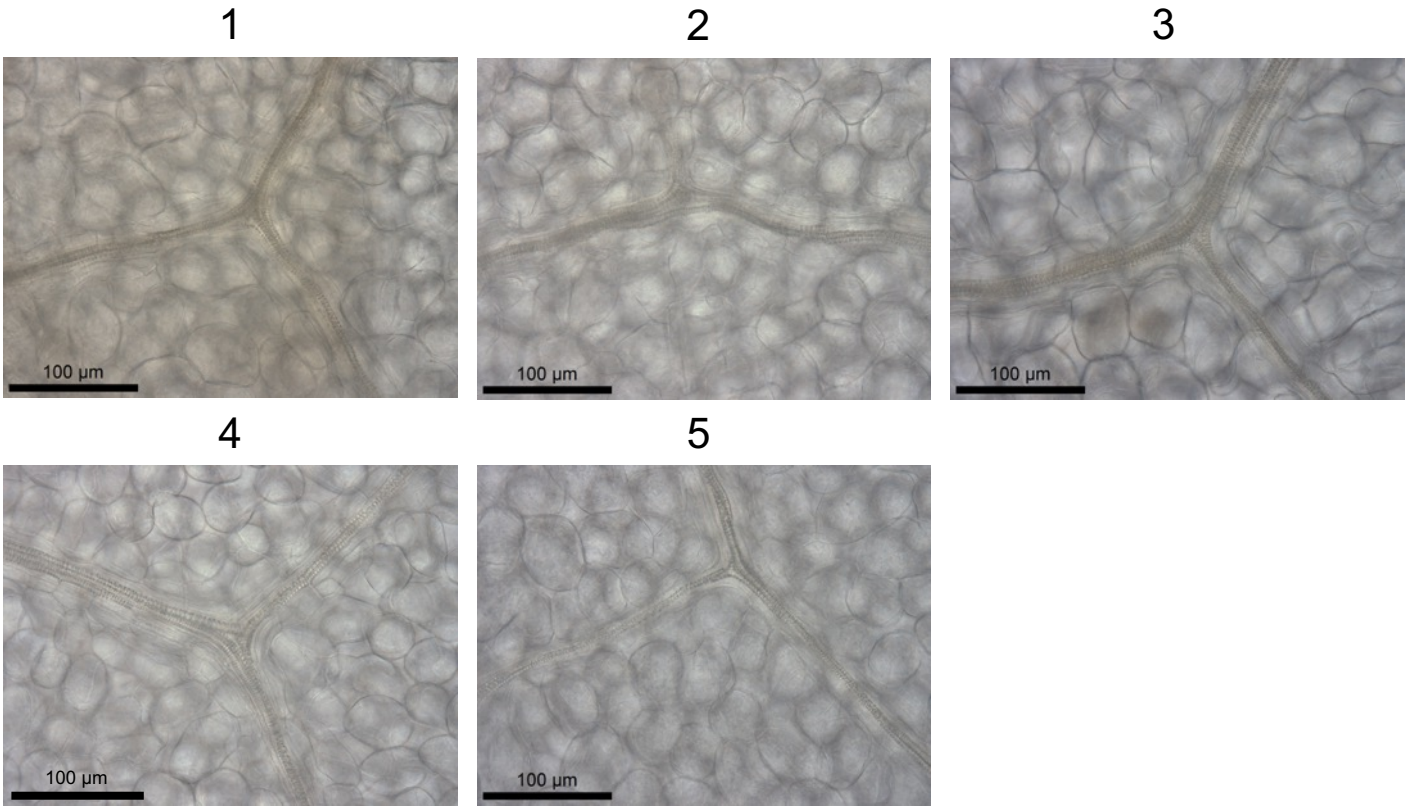

b

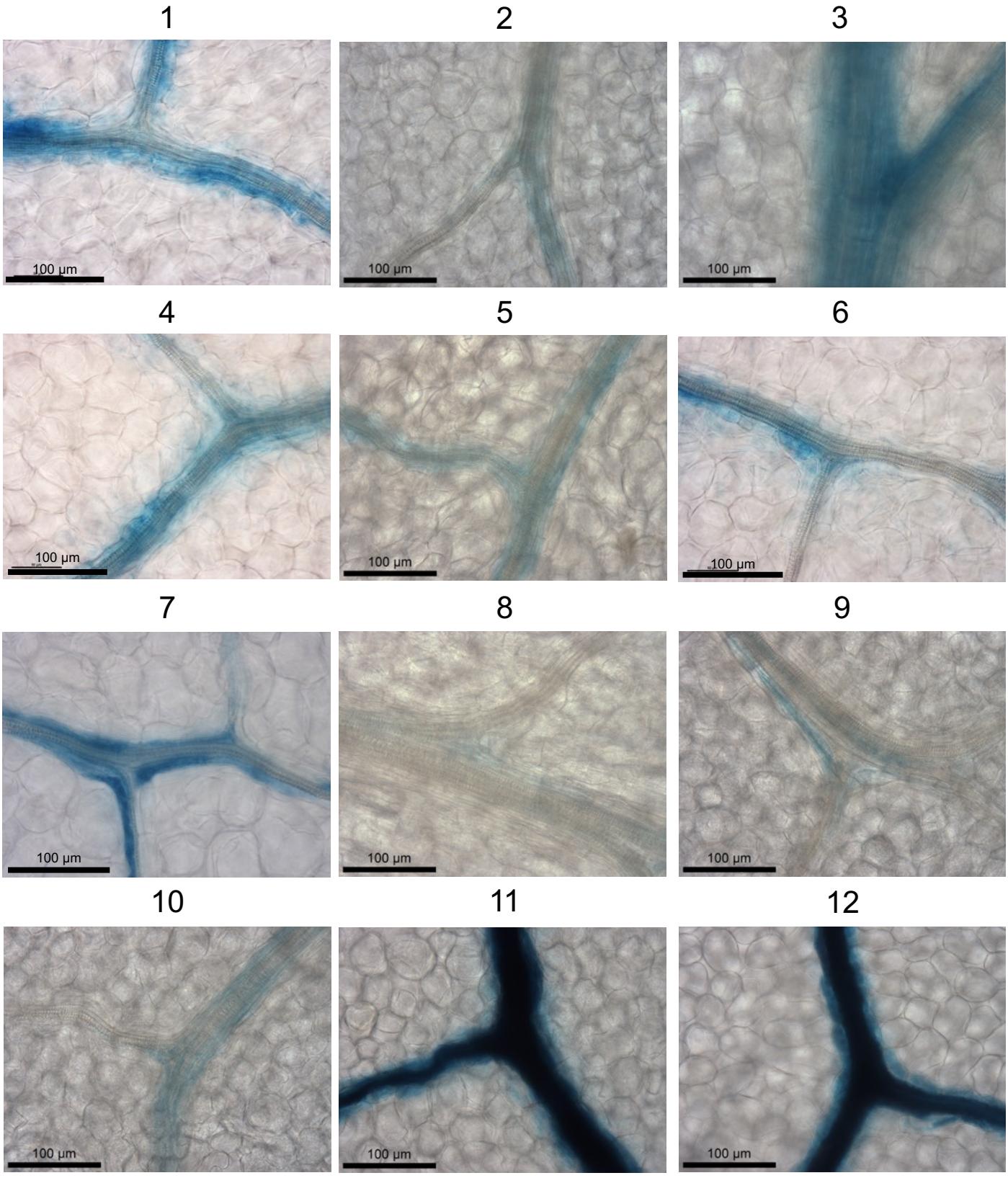

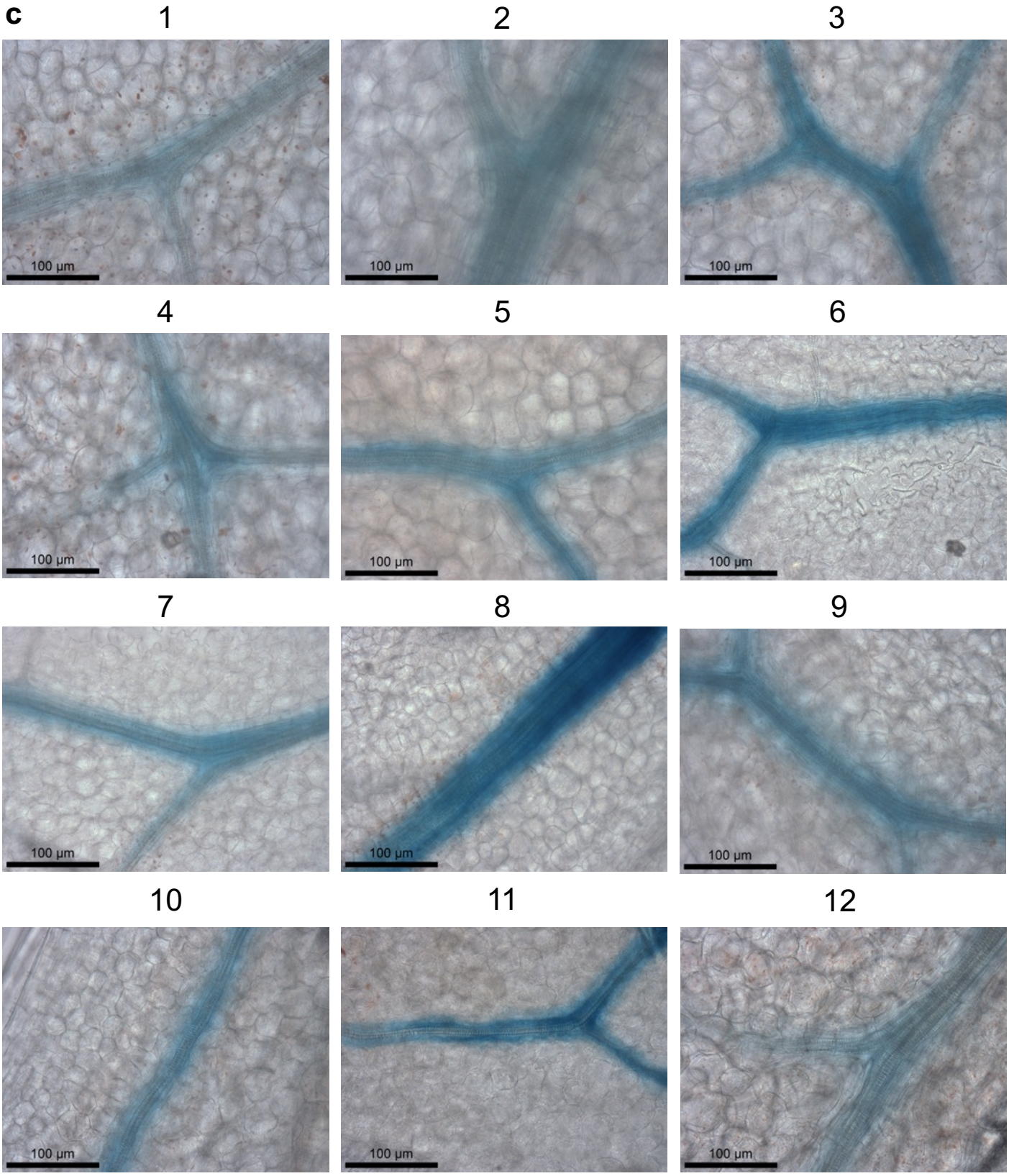

Supplementary Figure 7: a) Deleting the MYB76 DHS leads to loss of GUS in the BS. Images from 5 independent transgenic lines, leaves were stained for 48 hrs. b) The *MYB76* DHS combined with the minimal 35SCaMV promoter generates preferential expression in the bundle sheath. Images from 12 independent transgenic lines. Leaves were stained for 72hrs. c) Oligomerizing the *MYB76* DHS combined with the minimal 35SCaMV promoter generates strong preferential expression in the bundle sheath. Images from 12 independent transgenic lines. Leaves were stained for 3hrs. Scale bars represent 100 µm.

a

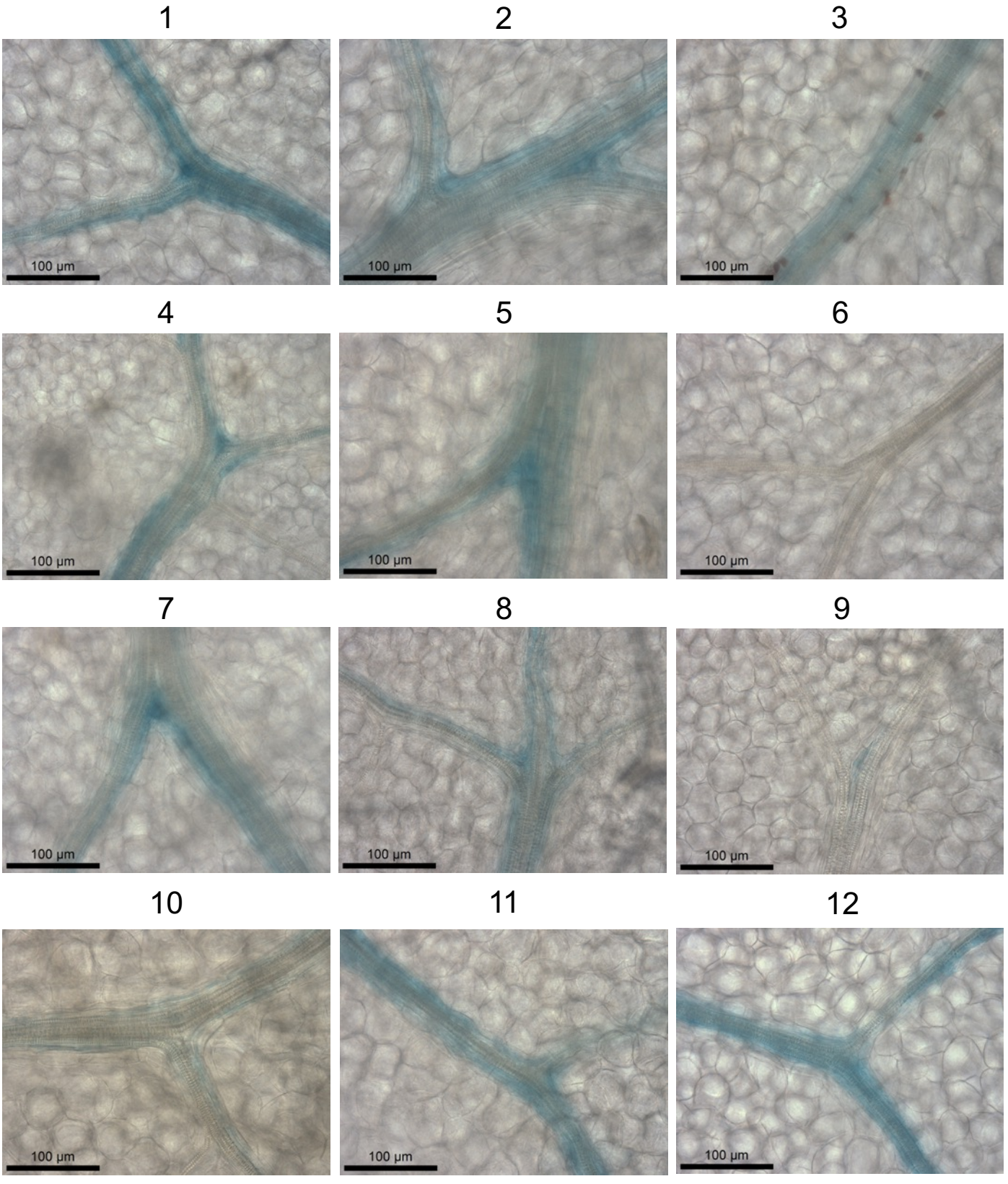

b

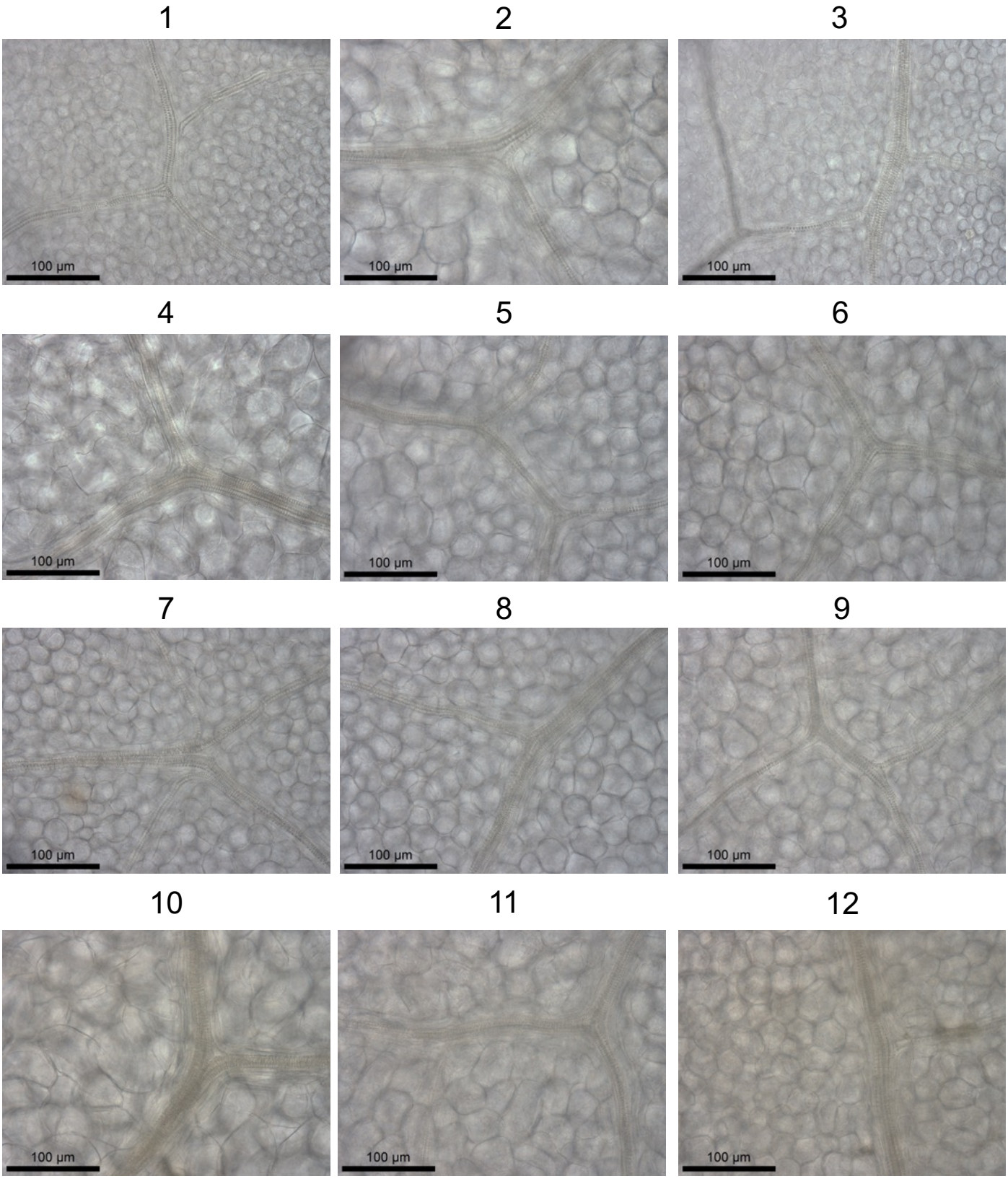

c

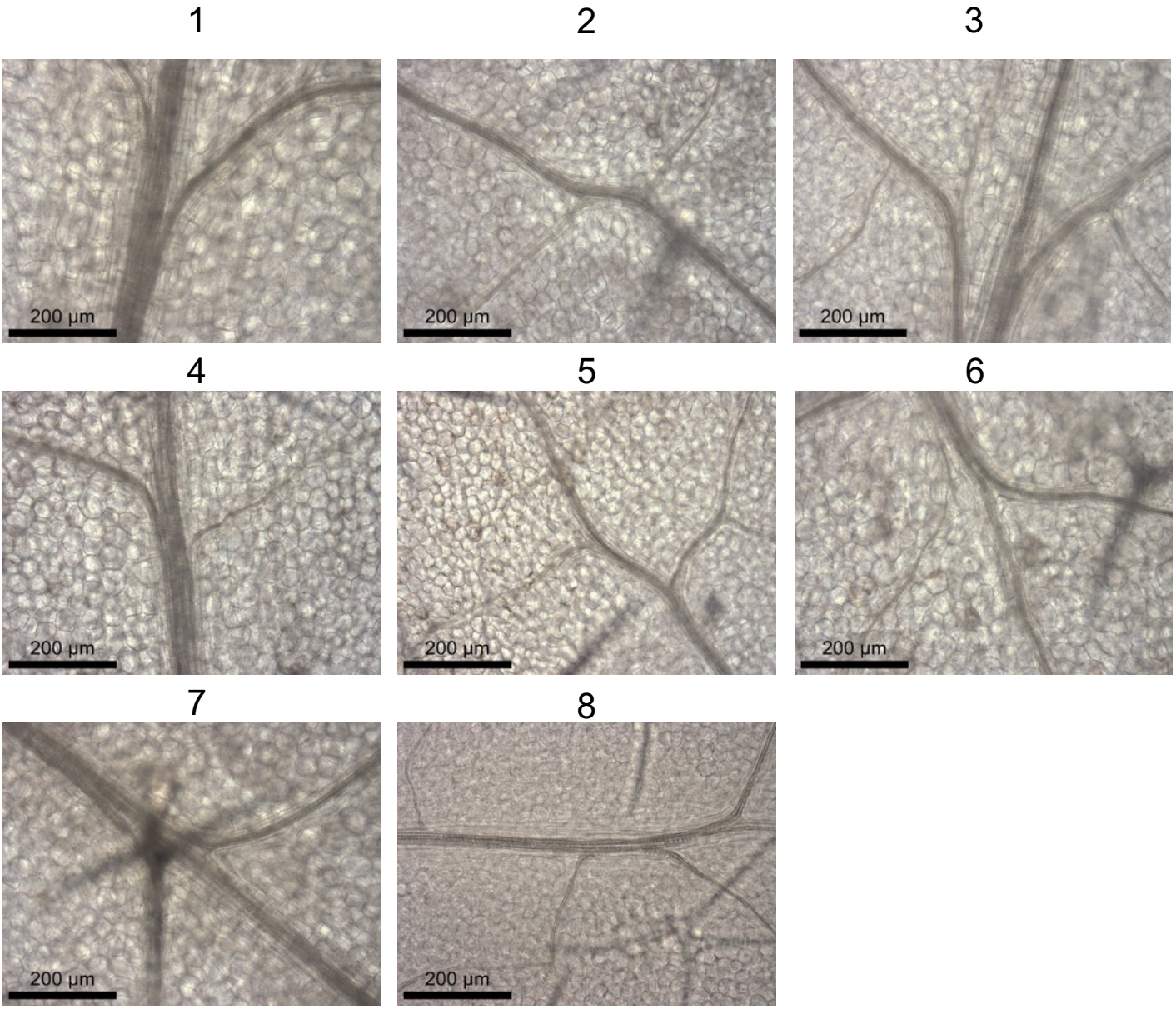

Supplementary Figure 8: a) Mutation of motif 1 (TGGGCA) from the *MYB76* promoter does not abolish accumulation of GUS from the bundle sheath. Images from 12 independent transgenic lines. Leaves were stained for 48hrs. b) Mutation of motif 2 (TGCACCG) from the *MYB76* promoter motif leads to loss of GUS in the BS. Images from 12 independent transgenic lines. Leaves were stained for 48hrs. Scale bars represent 100 µm. c) Mutation of the predicted MYC binding site (AAACGTG) from the DHS abolishes GUS accumulation. Images from 8 independent transgenic lines. Leaves were stained for 48hrs. Scale bars represent 200 µm.

a

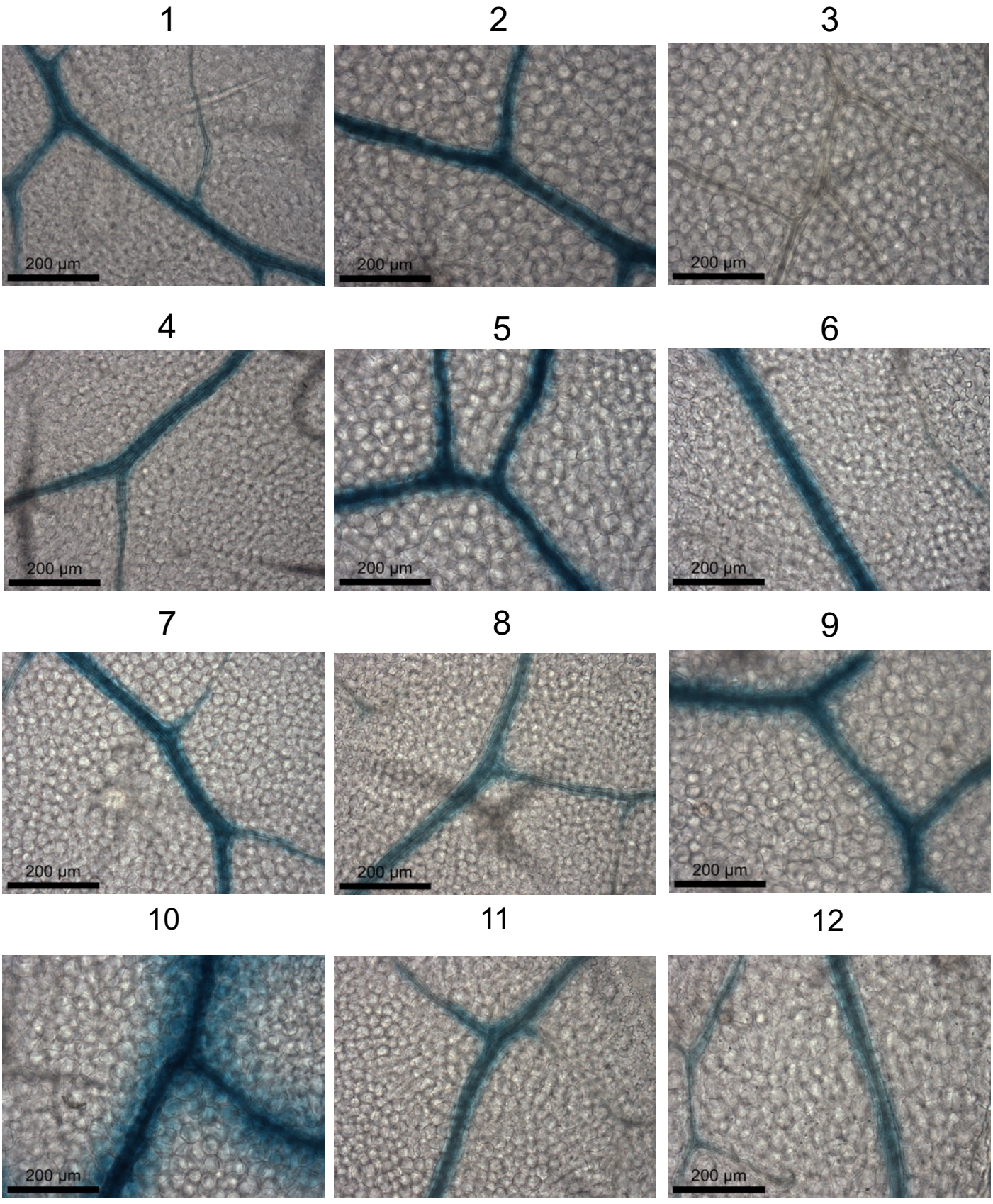

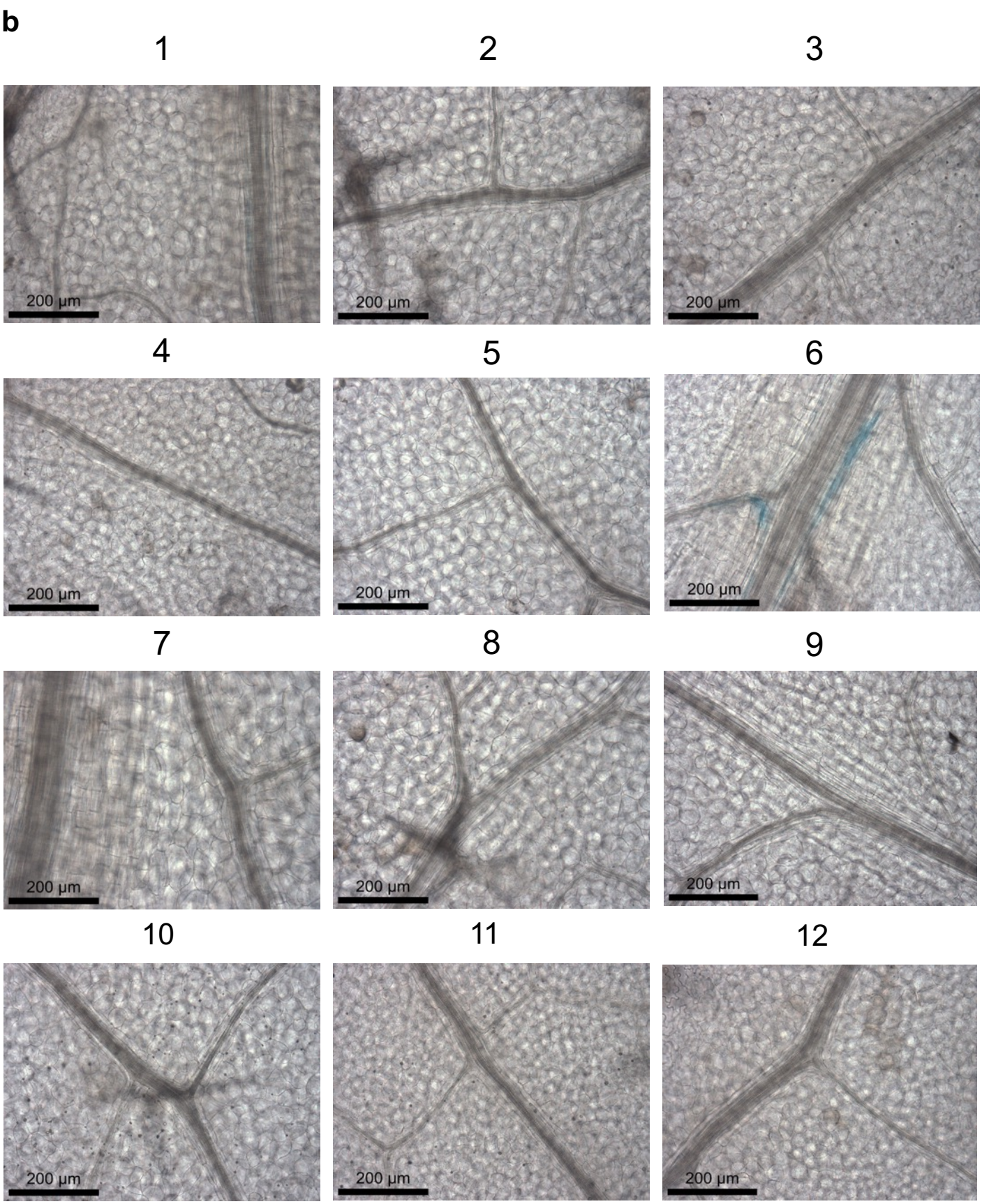

Supplementary Figure 9: a) *MYB76* promoter and *gDNA* fused to GUS generated using Golden Gate cloning generates preferential expression in the bundle sheath. Images from 12 independent transgenic lines. b) Mutation of motif 2 (TGCACCG) in a full length *MYB76* promoter and gDNA translational fusion abolishes GUS accumulation. Images from 12 independent transgenic lines. Leaves were stained for 24 hrs. Scale bars represent 200 µm.

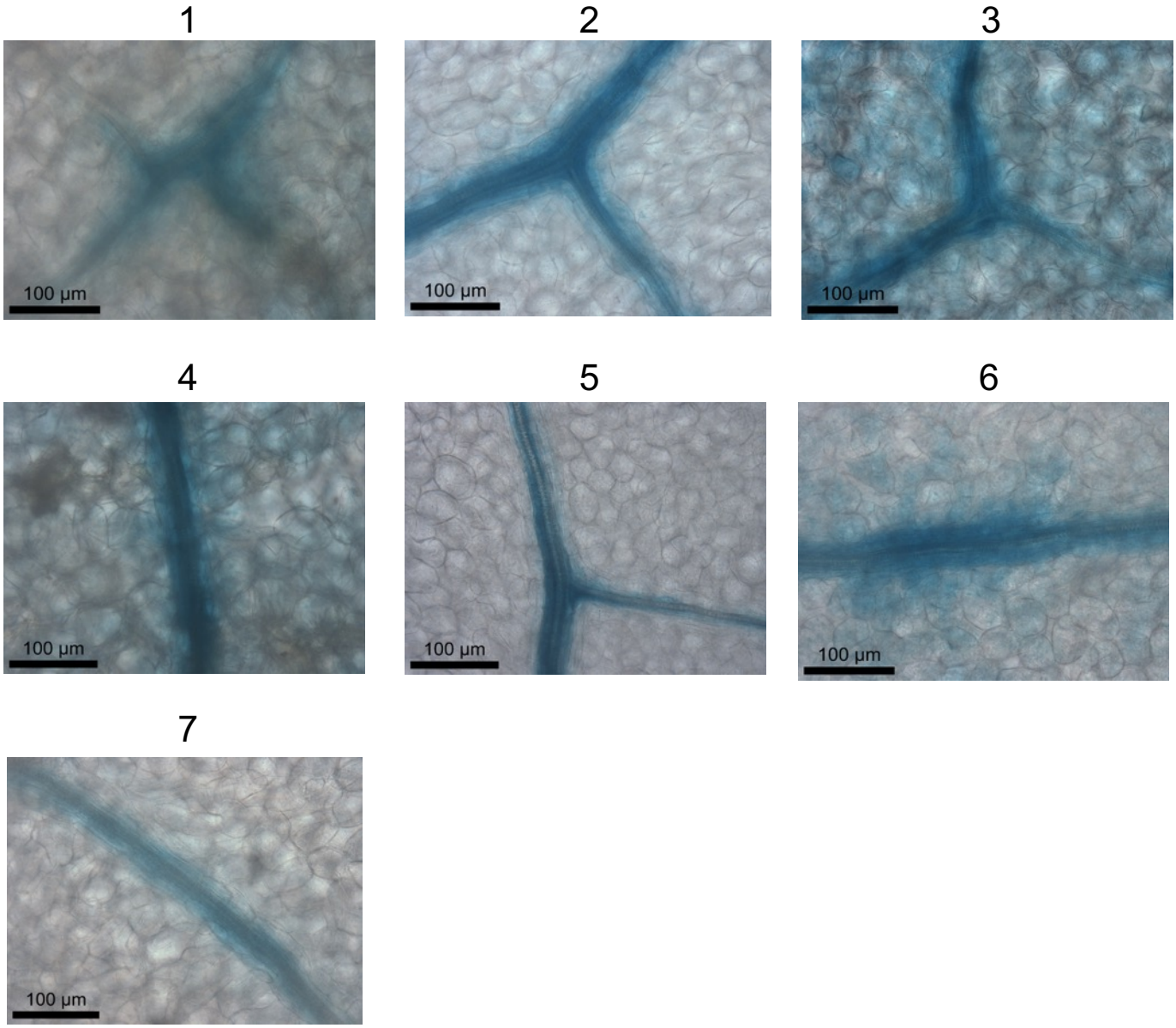

Supplementary Figure 10: Two copies of the TGCACCG motif combined with ten upstream and ten downstream nucleotides within the context of the native *MYB76* promoter fused to the minimal 35SCaMV minimal promoter generate preferential expression in the bundle sheath. Images from 7 independent transgenic lines. Leaves were stained for 86hrs. Scale bars represent 100 µm.

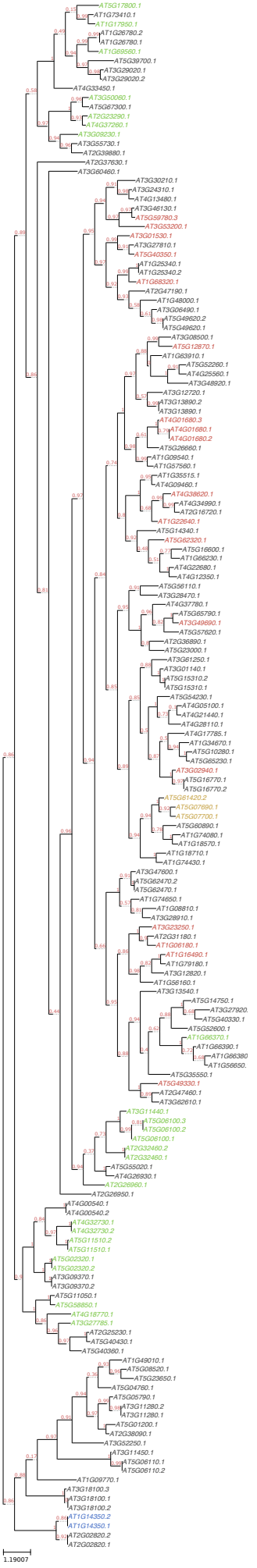

Supplementary Figure 11. Phylogenetic tree of MYB transcription factors in *A. thaliana* based on amino acid sequence of whole proteins. Cluster 10 MYBs are coloured in green, cluster 18 MYBs are coloured in red and cluster 31 MYBs are coloured in blue. MYB transcription factors without defined binding motifs are in black and MYB28, MYB29 and MYB76 are coloured in gold.

a

JASPAR id	TF	start	stop	strand	score	p-value	q-value	matched sequence	motif centre	Cluster
UN0355.1	AT3G49930	136	146	+	13.0504	1.51E-05	0.00734	TATACCTAATT	141	18
MA1042.1	MYB59	138	145	-	11.7563	6.48E-05	0.0316	ATTAGGTA	141.5	18
MA1293.1	MYB57	136	149	+	13.7656	1.31E-05	0.0063	TATACCTAATTTCC	142.5	18
MA1292.1	MYB27	136	150	-	16.5938	1.97E-06	0.000951	AGGAAATTAGGTATA	143	18
MA1294.1	MYB62	137	151	-	12.7031	2.86E-05	0.0138	AAGGAAATTAGGTAT	144	18

b

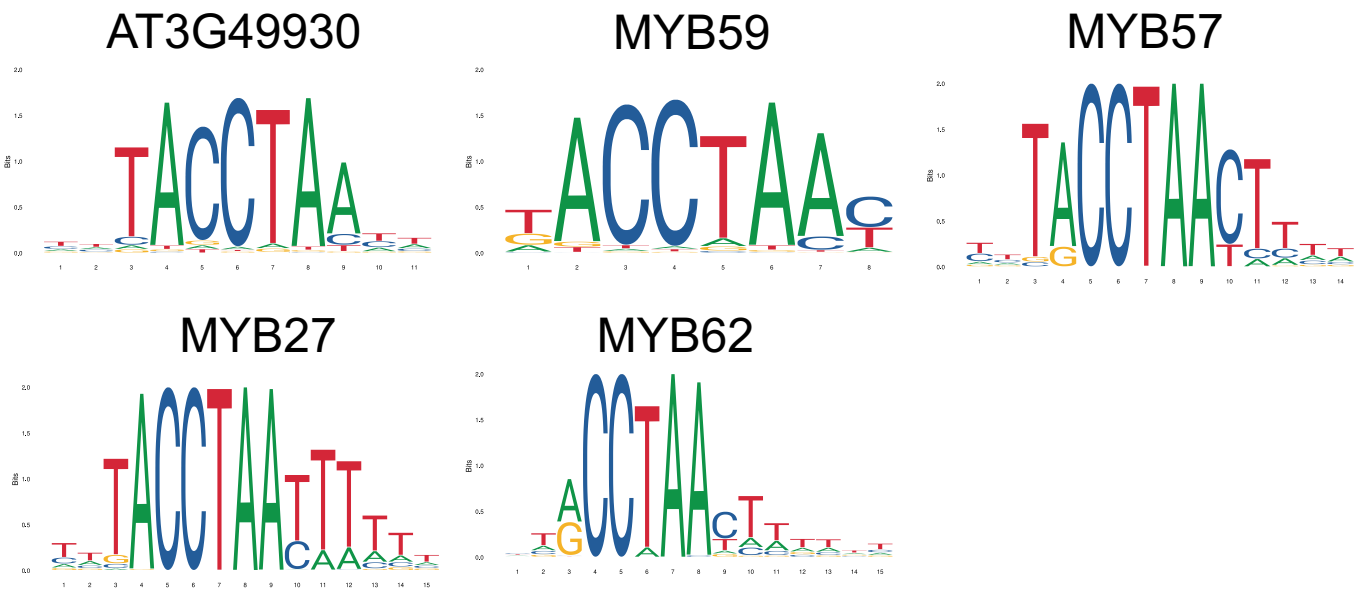

c

GATGATAACACCTGAATTTAATGACAAAAAAAAAAAAAAGTGGATAGAG
ACTAGAGGGACAGCAAGGCTGTGTGACATATATGGGCAGATAGACAAA
GAAGCCGAAAAACGTGCACCGTCCAAGATTCTGGCTACTATACCTAATTT
CCTTCCCGCAGGGACTTGACAAATATCACTATCTGCCATTTTTAGTTTTAT
TTTGTATTGGTGTCAAAGAATTGAAATAATGAACAACGGTCGTAAAAAGA
TGTAAATG

Supplementary Figure 12. Cluster 18 MYB transcription factor binding sites in the *MYB76* DHS. a) FIMO output showing matches to cluster 18 MYBs in the *MYB76* DHS. The *MYB76* DHS was used as the input sequence and all Arabidopsis motifs in the JASPAR database were used as input motifs. Output filtered for matches to cluster 18 MYBs. p-values calculated from log-likelihood score by the FIMO tool (Grant et al., 2011). b) Visualisations of Position Weight Matrices for the cluster 18 motifs found in the *MYB76* DHS. The orientation of the motif is shown as that found in the 5' to 3' direction on the DHS. c) Sequence of the *MYB76* DHS with the MYC binding site (gold) and conserved cluster 18 MYB binding site (blue) annotated.

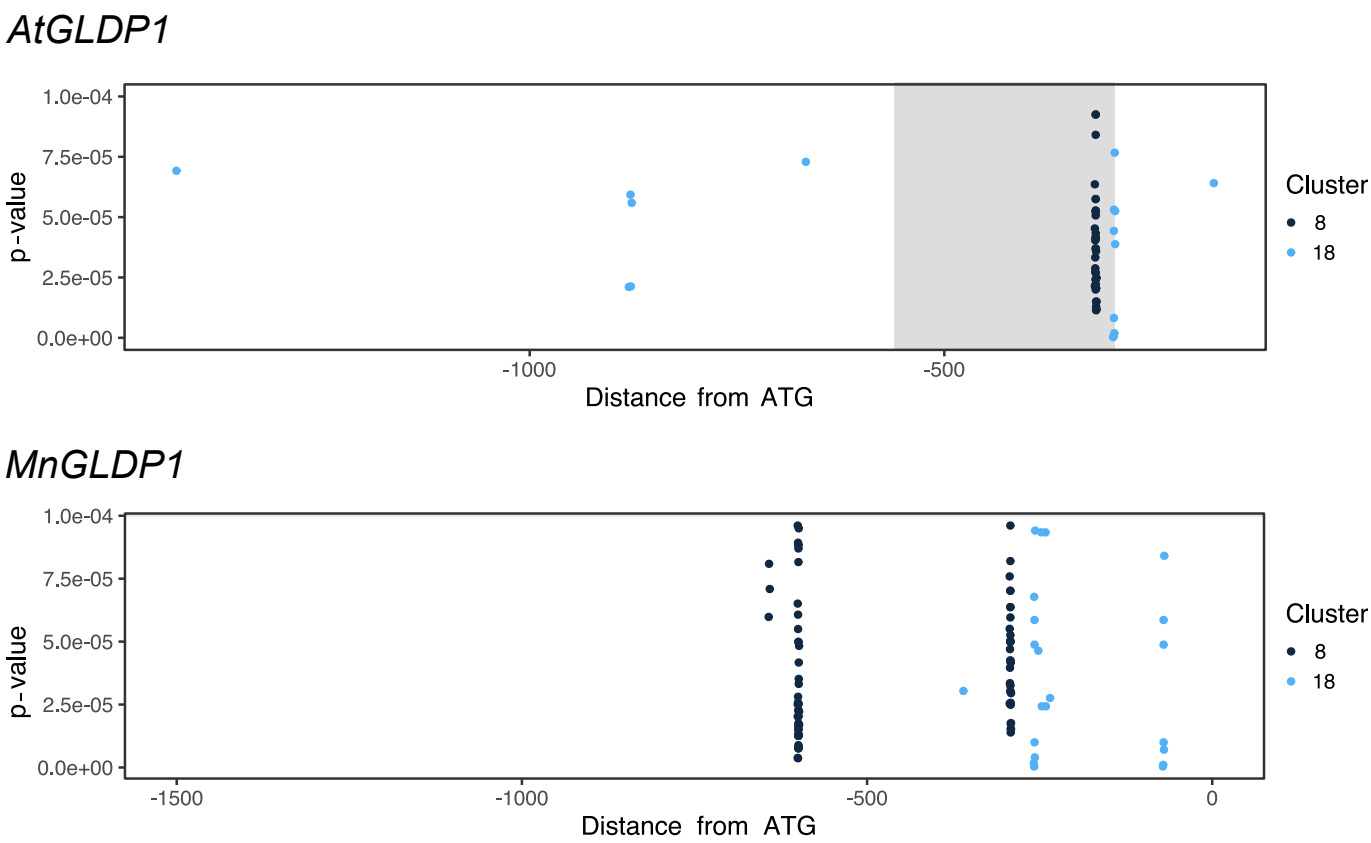

Supplementary Figure 13. Cluster 8 and 18 transcription factor binding motifs within the promoters of *A. thaliana* and *M. nitens GLDP1* genes. The y axis shows p-values of matches between DHS sequence and motif PWMs and the x axis shows position of the motif centre relative to the translational start site. p-values calculated from log-likelihood score by the FIMO tool (Grant et al., 2011). The grey box in the *AtGLDP1* promoter represents the V-box (Adwy et al., 2015).